10th IAEA TM on "H-mode Physics and Transport Barriers"
St. Petersburg, Russia
2005/09/28-30

Improved Confinement
projections/issues for burning devices

Atsushi FUKUYAMA
Department of Nuclear Engineering
Kyoto University

in collaboration with
K. Itoh, S.-I. Itoh, M. Yagi
and contributors of this Workshop

OUTLINE

- **Overview**
  - **Introduction**
  - **Scaling issues**
  - **Modeling issues**
- **Summary**

- **Discussion on Remaining Issues**
  - **Scaling** Y. Kamada
  - **Modeling** V. Rozhansky
  - **Improved confinement** E.J. Doyle

Requirements for Burning Devices

- **Requirements of Improved Confinement for Burning Plasma**
  - High energy confinement
  - High density
  - High normalized β
  - High bootstrap current
  - High non-inductively driven current
  - High fuel purity
  - High radiation power
  - Low peak power flux to divertor

Improved Confinement

- **Various kinds of improved confinement**
  - ETB Indispensable for high Q operation
  - ITB Beneficial for long time operation
  - Plasma rotation, Impurity injection, etc.

- **Results of closely coupled transport phenomena**

- **Reliable Scaling and Modeling of improved confinement are necessary for projection to burning devices.**

Model of ITB Formation

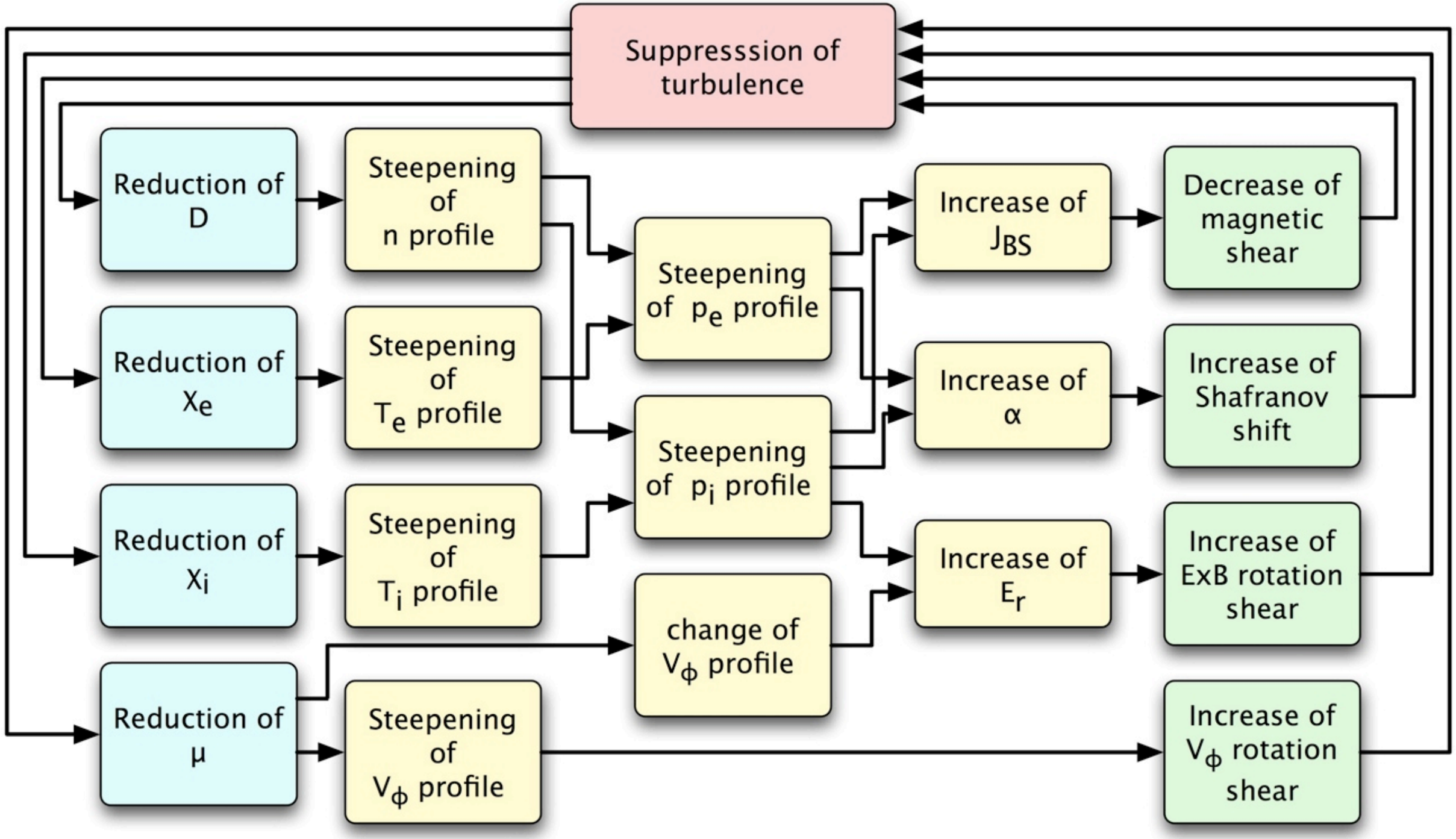

Scaling

- **Global confinement scaling**
  - L-mode scaling
  - H-mode scaling
    - β scaling (Takizuka, Kaye)
    - R/a scaling (Kaye)
    - 1.5D ITER Simulation (Polevoi)
  - Density profile scaling (Weisen)

- **Edge plasma scaling**
  - L-mode density limit (Greenwald limit)
  - H-mode density limit
    - Borrass scaling: $n_{BLS} = q_{\perp}^{0.094} B^{0.53} (q_{95} R)^{-0.88}$
  - Pedestal stability scaling
    - δ dependence -> Total β_p scaling (Kamada)
    - Pedestal temperature scaling (Onjun)
  - H-mode power threshold scaling (McDonald)

T. Takizuka: Origin of the various beta dependence of ELMy H-mode confinement properties

IPB98(y,2)

$$\tau_{th,98y2} = 0.0562\, I_p^{0.93} B_t^{0.15} n_{19}^{0.41} P_L^{-0.69} R^{1.97} \varepsilon^{0.58} \kappa_a^{0.78} M^{0.19}$$

$$\tau_{th,98y2} \propto \tau_B\, \rho_*^{-0.7}\, \beta^{-0.9}\, \nu_*^{-0.01}$$

Two term model

$\tau_E\ (\equiv W/P_L) = \tau_{core}/(1-\beta_{ped}/\beta)$ (MHD limited β_{ped} independent of P_L)

Non-dimensional transport experiments in JET and DIII-D

$$\tau_{th}/\tau_B \propto \beta^0$$

NF following 20th IAEA FEC (Cordey)

Standard set (OLS-R)

$$\tau_{th,04(1)} = 0.0596\, I_p^{0.86} B_t^{0.21} n_{19}^{0.40} P_L^{-0.65} R^{2.00} \varepsilon^{0.69} \kappa_a^{0.84} M^{0.08}$$

$$\tau_{th,04(1)} \propto \tau_B\, \rho_*^{-0.8}\, \beta^{-0.66}\, \nu_*^{-0.09}$$

ITER-like subset

(OLS-R) $\tau_{th,04(2a)} = 0.096\, I_p^{1.06} n_{19}^{0.39} P_L^{-0.61} R^{1.78} \varepsilon^{0.56}$

$$\tau_{th,04(2a)} \propto \tau_B\, \rho_*^{-0.89}\, \beta^{-0.38}\, \nu_*^{-0.31}$$

(EIV-R) $\tau_{th,04(2b)} = 0.0933\, I_p^{1.00} n_{19}^{0.37} P_L^{-0.55} R^{1.73} \varepsilon^{0.56}$

$$\tau_{th,04(2b)} \propto \tau_B\, \rho_*^{-0.78}\, \beta^{-0.20}\, \nu_*^{-0.20}$$

T. Takizuka:

Analysis of JT-60U Data (2000~2002 Experiments)

H-mode, high-density H-mode and High β_p H-mode

Searching out 3 suitable datasets with the same ρ_* and ν_* values

(R/a ~ 3.3m/0.8m, κ ~ 1.4, δ ~ 0.4, q_{95} ~ 4)

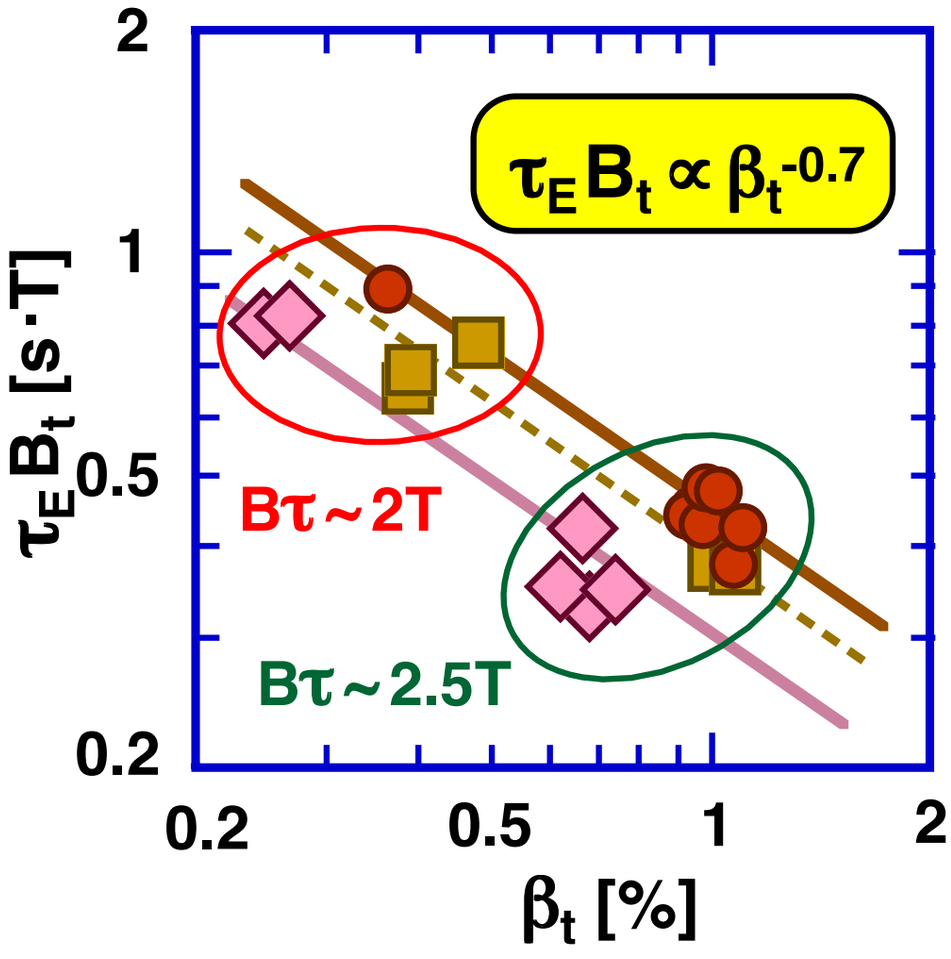

Clear degradation of τ_E with high β is seen for ELMy H-mode in JT-60

(τ_E: global energy confinement time)

H Urano, T. Takizuka, H. Takenaga, N. Oyama, Y. Miura, Y. Kamada, "Confinement Degradation with Beta for ELMy H-mode Plasmas in JT-60U Tokamak ", Submitted to Nucl. Fusion.

SUMMARY

- Common conclusion for β dependence of ELMy H-mode confinement has not been obtained.
- Recent non-dimensional transport experiments in JT-60U demonstrated clearly the β degradation.
- Strong β degradation consistent with above experiments is confirmed by the analysis of JT-60U database.
- Two subsets of AUG and JET data in the ITPA database are analyzed to find the origin of various beta dependences.
- Shaping, e.g., δ_{upper} and κ, affects confinement performance, and resultantly causes the variation of β dependence.
  AUG low δ_{upper} : strong β degradation
  JET w/o gas puff : no β degradation

Essential factor in shaping and Physics mechanism for changing β dependence are future issues to be solved.

S. Kaye: The Role of Aspect Ratio and Beta in H-mode Confinement Scalings

NSTX, MAST and START Data Significantly Extend the Range of Both β and ε

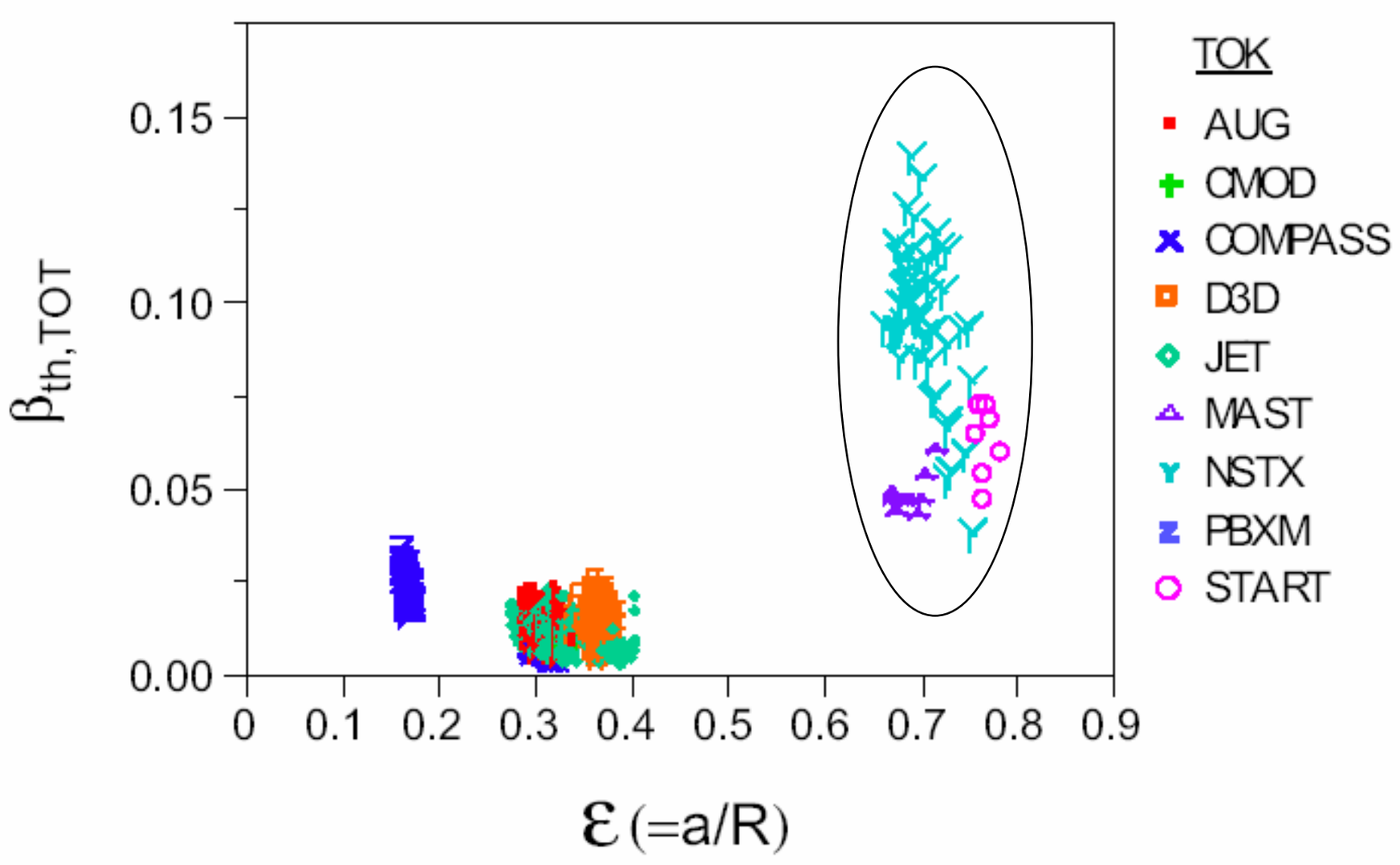

- *β–ε correlation introduced*

S. Kaye: # IPB98(y,2) Scaling Overestimates Confinement at Low R/a (H<1)

$$\tau_{E,th}^{IPB98(y,2)} \sim I_p^{0.93}\, B_T^{0.15}\, n_e^{0.41}\, P_{L,th}^{-0.69}\, \kappa^{0.78}\, M^{0.19}\, R^{1.97}\, \varepsilon^{0.58}$$

$$B\tau \sim \rho_*^{-2.7}\, \beta^{-0.9}\, \nu_*^{-0.01}$$

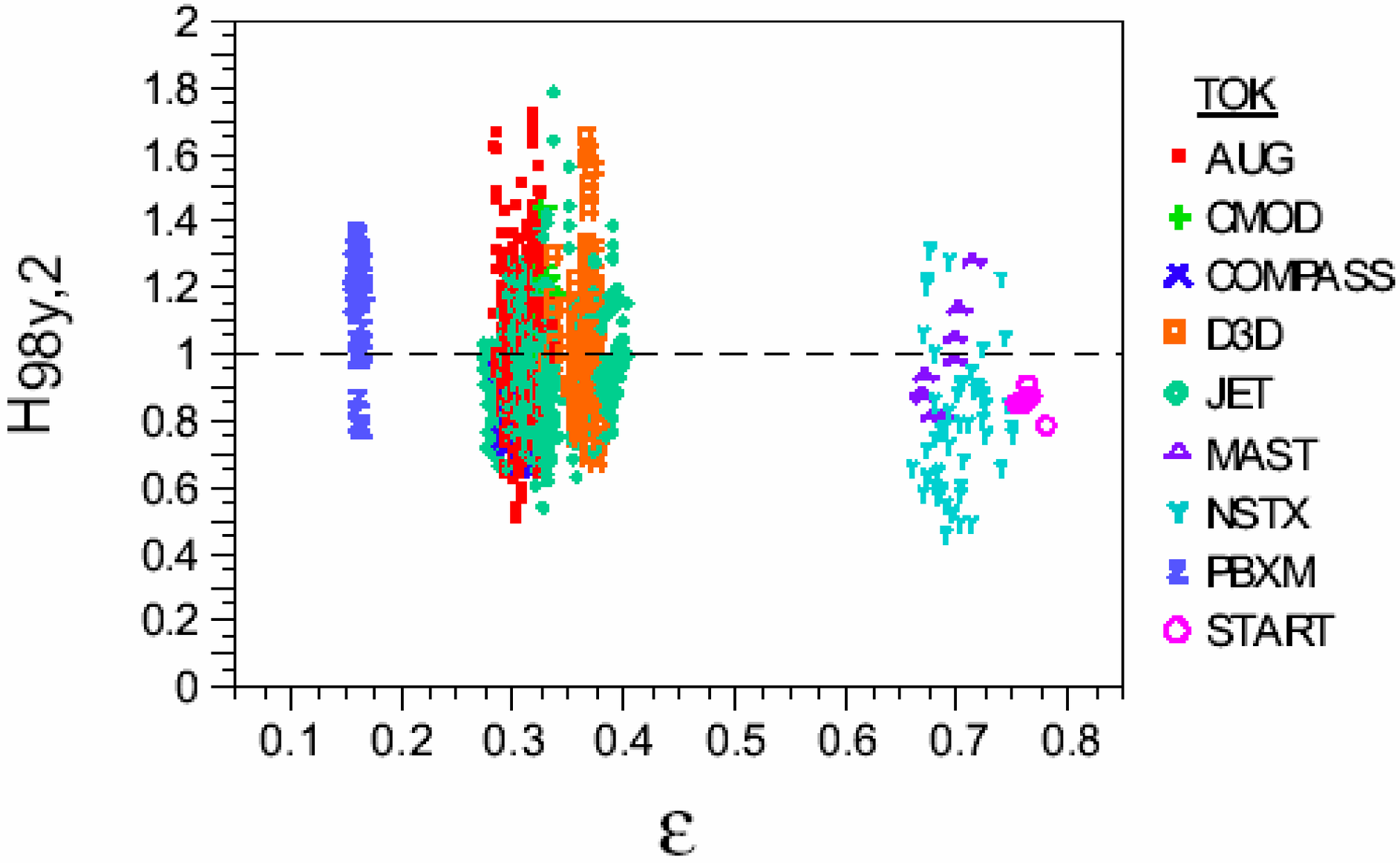

S. Kaye:

Conclusions

- Addition of high power, low aspect ratio data from NSTX and MAST has allowed for an investigation of the dependence of confinement on aspect ratio
- Dataset used for analysis is constrained by standard selection criteria in addition to shape and M_{eff}
- Low R/a data operate at low B_T, high β, so an inevitable correlation between β and ε exists in the dataset
- Fits based on engineering variables exhibit a stronger ε dependence than observed in scalings based only on devices with R/a>2.5
  - Transformation of these fits to physics variables indicate an unfavorable scaling of $B\tau$ on β

A.R. Polevoi: ITER Plasma Persormance Assessment on the Bases of Newly-proposed Scalings

Modeling of the ITER reference scenario with I_p = 15 MA with the newly proposed [1] scalings and y,2 scaling [2] was carried out with the 1.5D ASTRA transport code.

It is shown that for each scaling there is an operational window in the range of moderate densities n/n_G = 0.85 – 0.65 where the fusion power P_{fus} = 250-600 MW can be provided by neutral beam injection with power P_{NBI} = 16.5 MW + 16.5 MW and the ion cyclotron central heating with P_{ICR} = 0 - 20 MW.

In this operational window the fusion multiplication factor can reach the level Q = 10 – 20 even with a conservative assumption on helium transport: τ^*_α/τ_E = 5.

[1] J.G. Cordey, K. Thomsen, A. Chudnovskiy et al, Nucl Fusion 45 (2005) 1078-1084
[2] ITER Physics Basis, Nucl. Fusion 39 (1999) 2175.

A.R. Polevoi:

Comparison of ITER operational space predicted by ASTRA 1.5D simulations with different scalings. Revised scalings predictions mainly overlap with y,2 predictions.

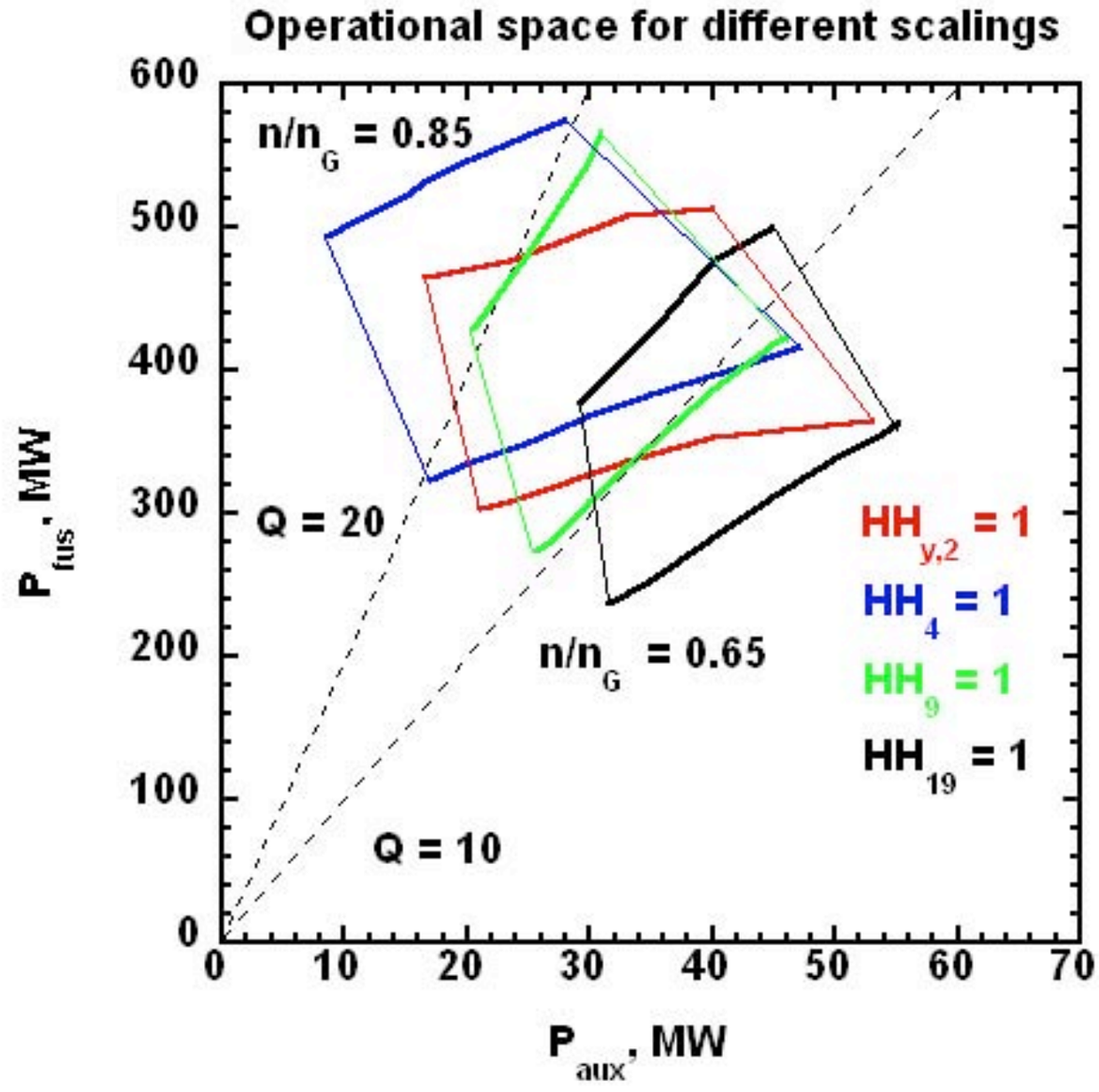

$$\tau_{E(y,2)} = 0.0562\, I^{0.93} B^{0.15} R^{1.97} n^{0.41} \varepsilon^{0.58} k^{0.78} M^{0.19} P^{-0.69},$$

$$\tau_{E(4)} = 0.0228\, I^{0.86} B^{0.21} R^{1.31} n^{0.4} a^{-0.99} A^{0.84} M^{0.08} P^{-0.65},$$

$$\tau_{E(9)} = 0.0198\, I^{0.85} B^{0.17} R^{1.21} n^{0.26} a^{-1.25} A^{0.82} M^{0.06} P^{-0.45},$$

$$\tau_{E(19)} = 0.088\, I^{0.9} R^{1.26} n^{0.3} a^{0.47} P^{-0.47}$$

A.R. Polevoi:

CONCLUSIONS

Revised scalings predict operational spaces for the ITER reference scenario which mainly overlap with y,2 predictions.

The fusion multiplication factor can reach the level Q = 10 – 20 even with a conservative assumption on helium pumping with $\tau^*_\alpha/\tau_E = 5$.

The operational space shrinks dramatically with the core particle confinement improvement and conservative scaling for LH power threshold. This is caused mainly by the increase of the fuel contamination by helium up to the 1.5-2.2 % in average.

Scalings 4, 9 and y,2(98) predict operation in the desirable range Q > 10 for $n/n_G = 0.85$ even in the case of the improved particle confinement.

J.H. Weisen: Scaling of density peaking in JET H-modes

Peaking decreases with ν_{eff}

- ICRH-only H-modes slightly below NBI H-modes on average
- ICRH modes at ITER collisionality have significant peaking

  Difference of low n_{eff} ICRH H-modes with ITER reference H-mode:
  β_N~1 and T_i/T_e~0.5

  ITER: β_N=1.8, T_i/T_e~0.9

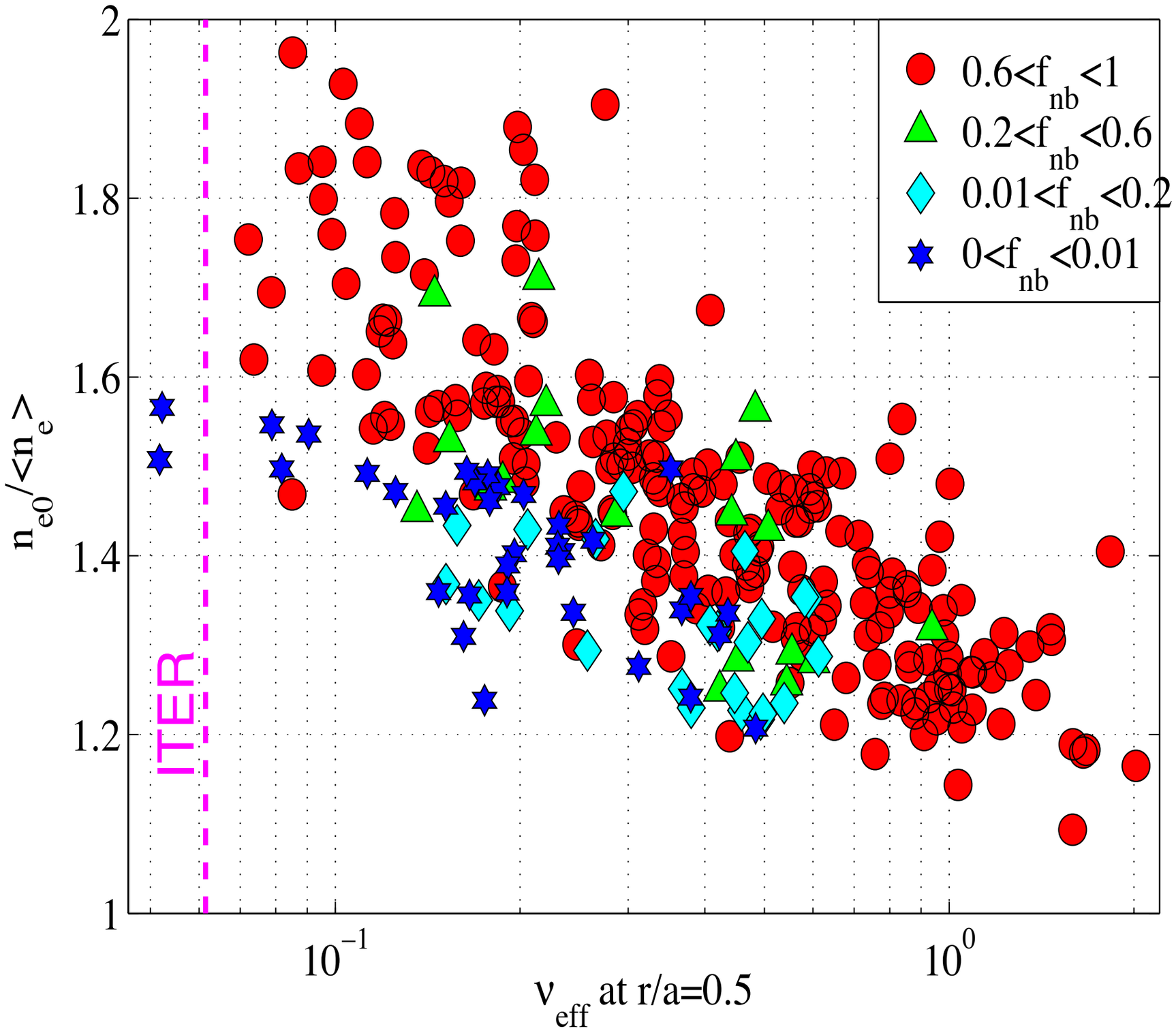

J.H. Weisen:

Peaking decreases with N_G

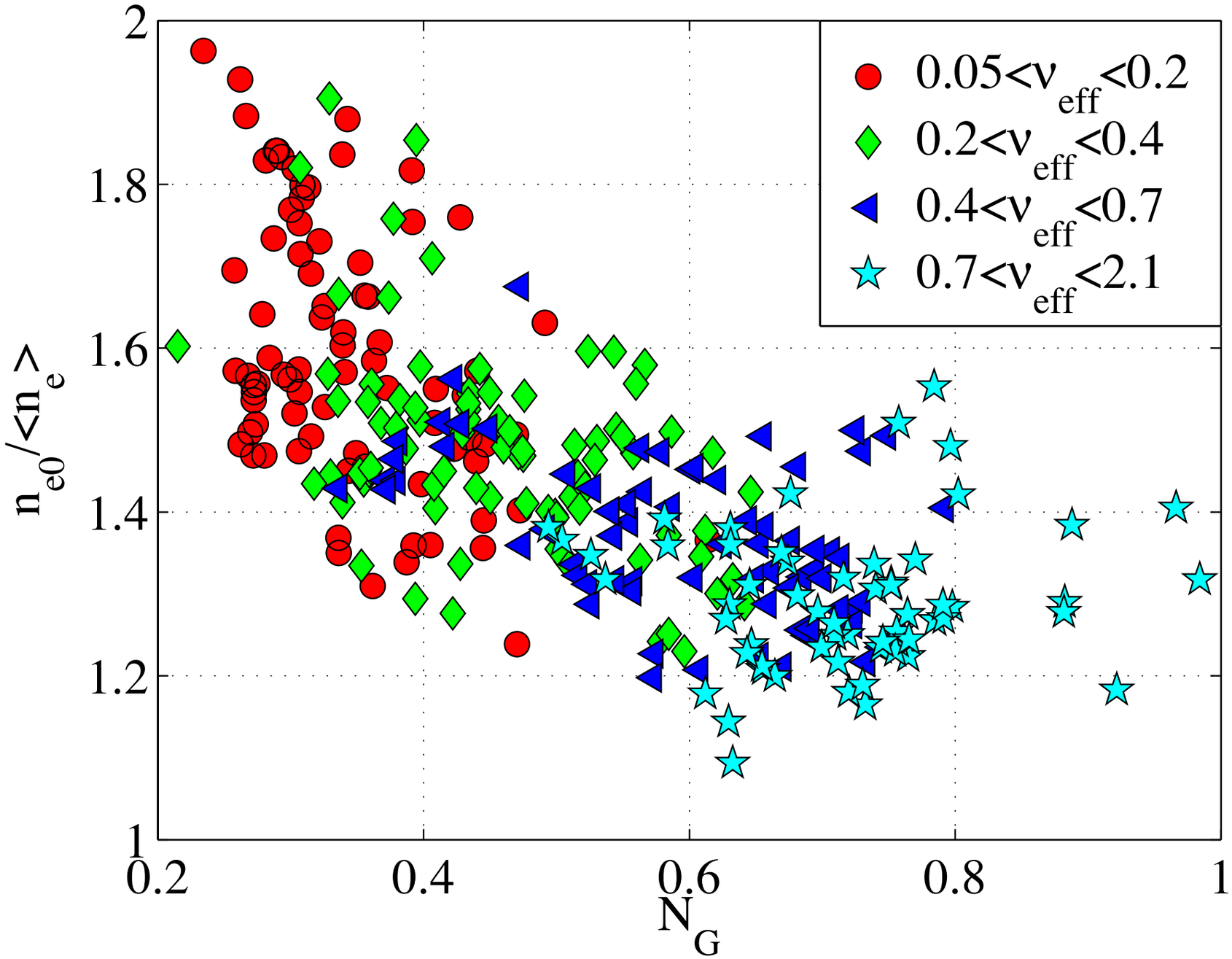

- Suggests very different (flat) extrapolation to ITER!

J.H. Weisen:

Conclusions

- Density peaking in H-modes is clearly anomalous
- NBI fuelling contributes modestly, as expected for $\chi/D \sim 1.5$
- Ware pinch contribution insignificant
- Dominant parameter dependencies on ν_{eff} (or ν^*), N_G, $\Gamma/n_e\chi$, T_i/T_e
- Weak, ambigous correlations with various measures of shear, q_{95}
- No dependence on $L_{Te}, L_{Ti}, \beta, \rho^*$
- Strong correlation of ν_{eff} and N_G, but N_G likely not to be appropriate
- Proposed best fits (local quantities at mid-radius):

$$R/L_{ne} = 0.78 - 1.28 \log_{10}\nu_{eff} + 1.28 R\Gamma/(n_e\chi) + 0.7 T_i/T_e \qquad \text{ITER: } 2.97$$

$$n_{e0}/\langle n_e \rangle = 1.09 - 0.34 \log_{10}\nu_{eff} + 0.2 R\Gamma/(n_e\chi) + 0.17 T_i/T_e \qquad \text{ITER: } 1.65$$

- Fusion power increase >30%, raises Q to >30
- Partial ‘insurance’ against possible low density limit

Y. Kamada: Impact of the Edge Pedestal Characteristics on the Integrated Performance in Advanced Operation Modes on JT-60U

2. Pedestal β_p increases with total β_p

At high-δ, pedestal β_p increases with β_p-total

(positive shear)

JT-60U

Pedestal pressure can be increased by x2 ~ 2.5.

Same tendency for standard H & ITB+H discharges.

(not the result of profile stiffness)

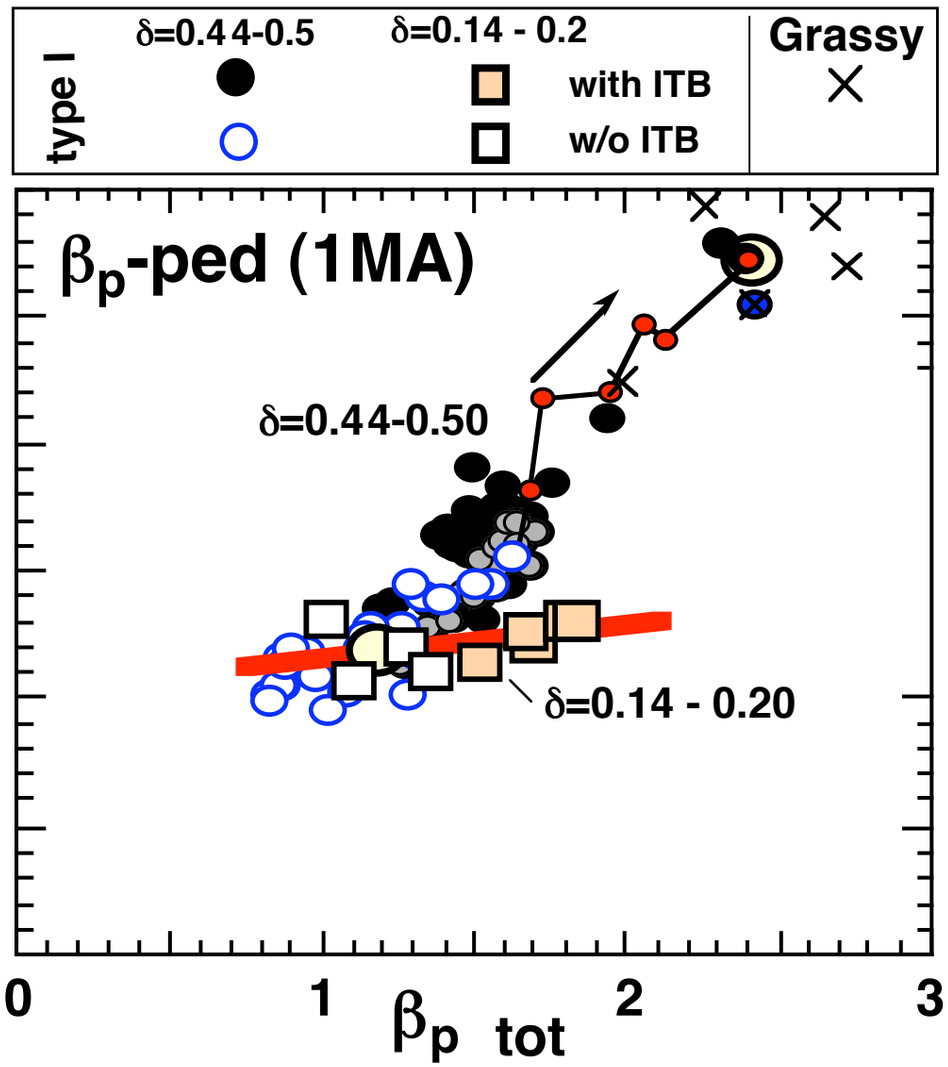

Y.Kamada,et al., Plasma Phys. Control. Fusion **44**, A279-A286, (2002).

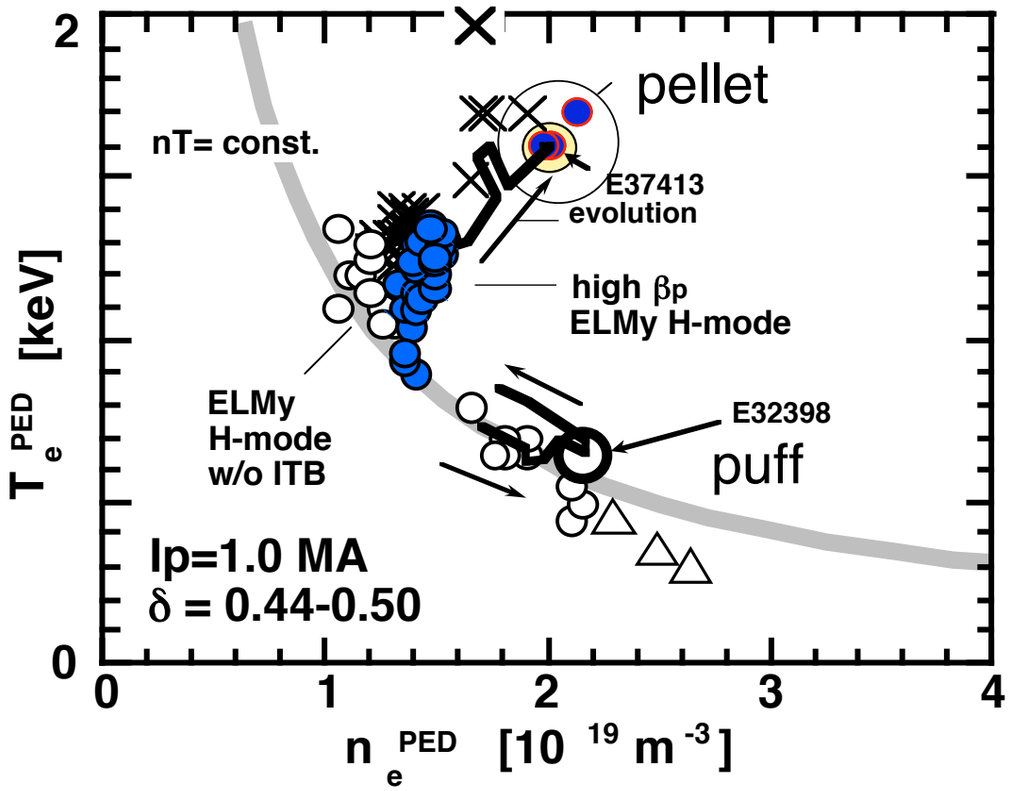

Y. Kamada:

RS ELMy H

JT-60U

Similar to the positive shear, βp-ped-max increases with δ, and βp-ped increases with βp-tot.
But, Ip=0.8MA cases has smaller βp-ped.

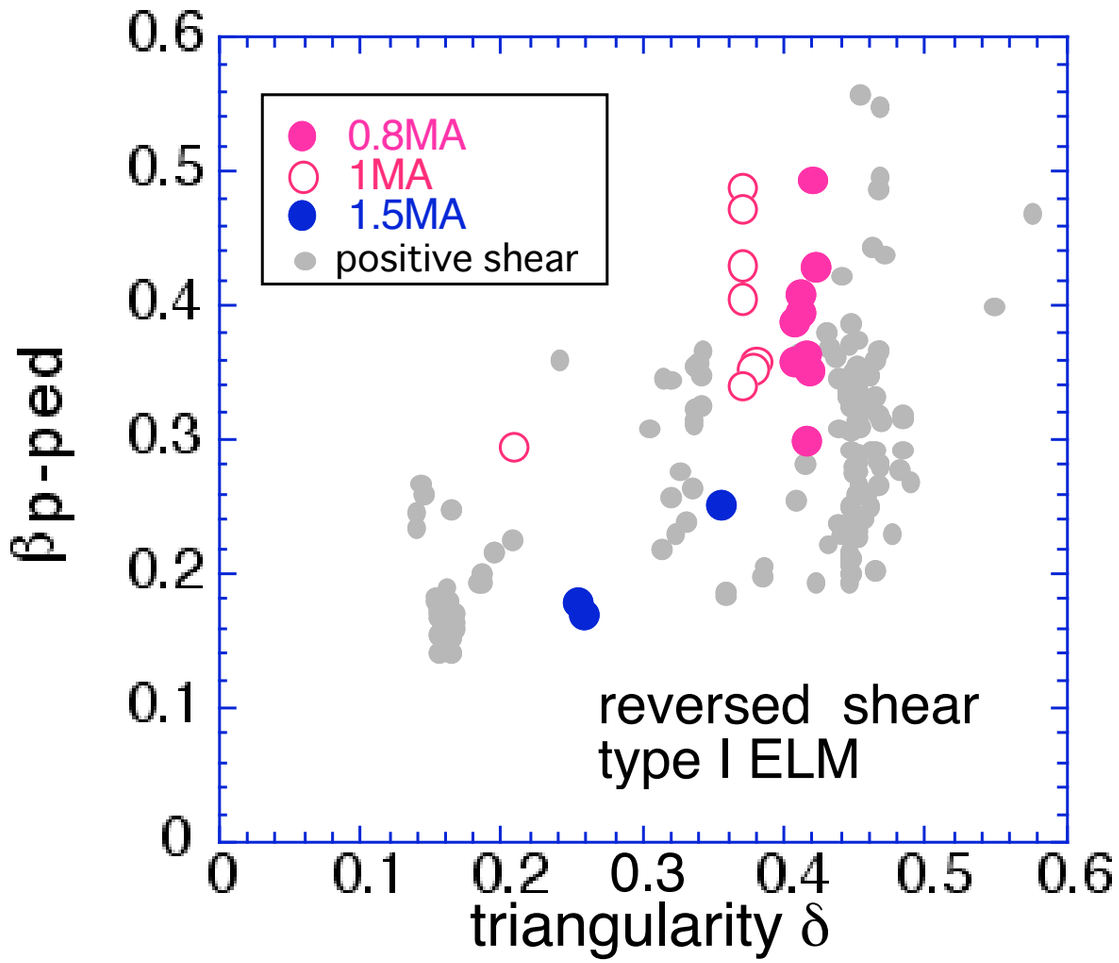

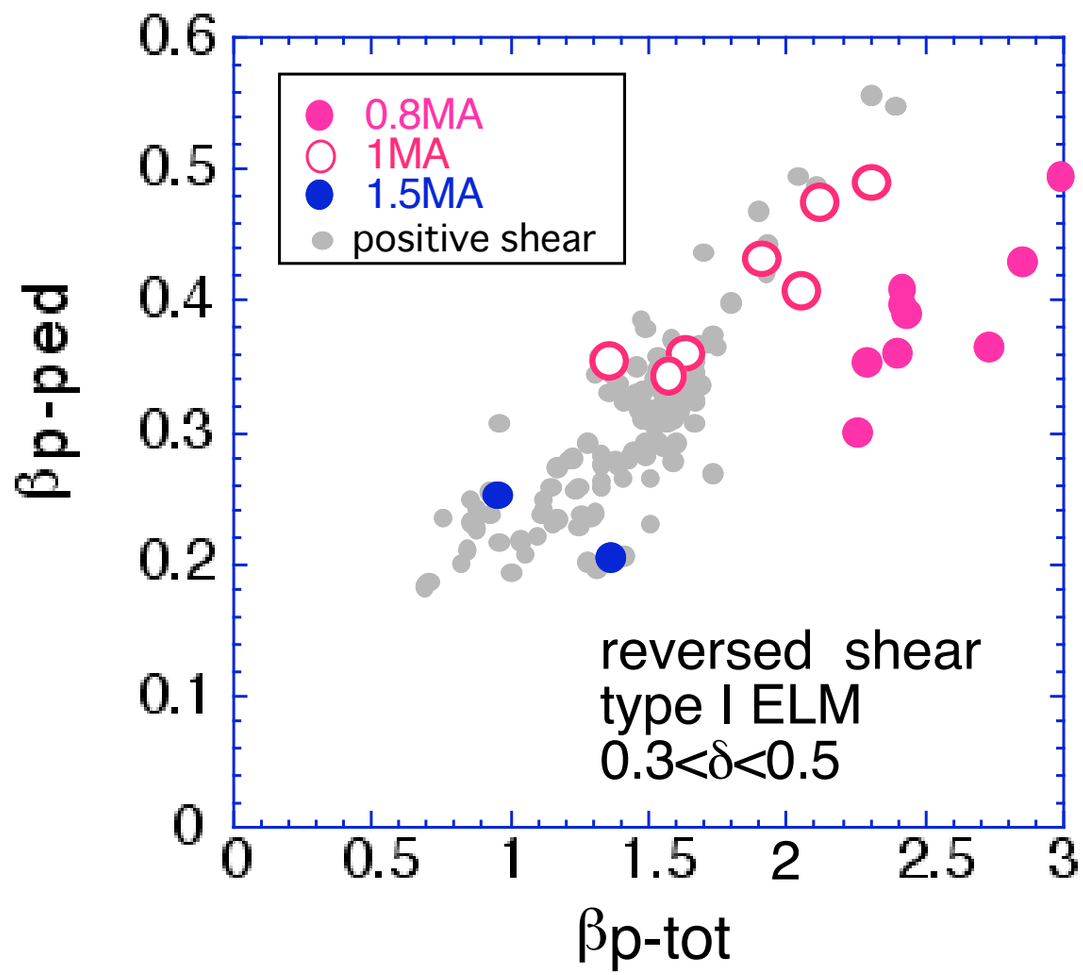

Y. Kamada:

ELM crash depth deepens with W-ped

JT-60U

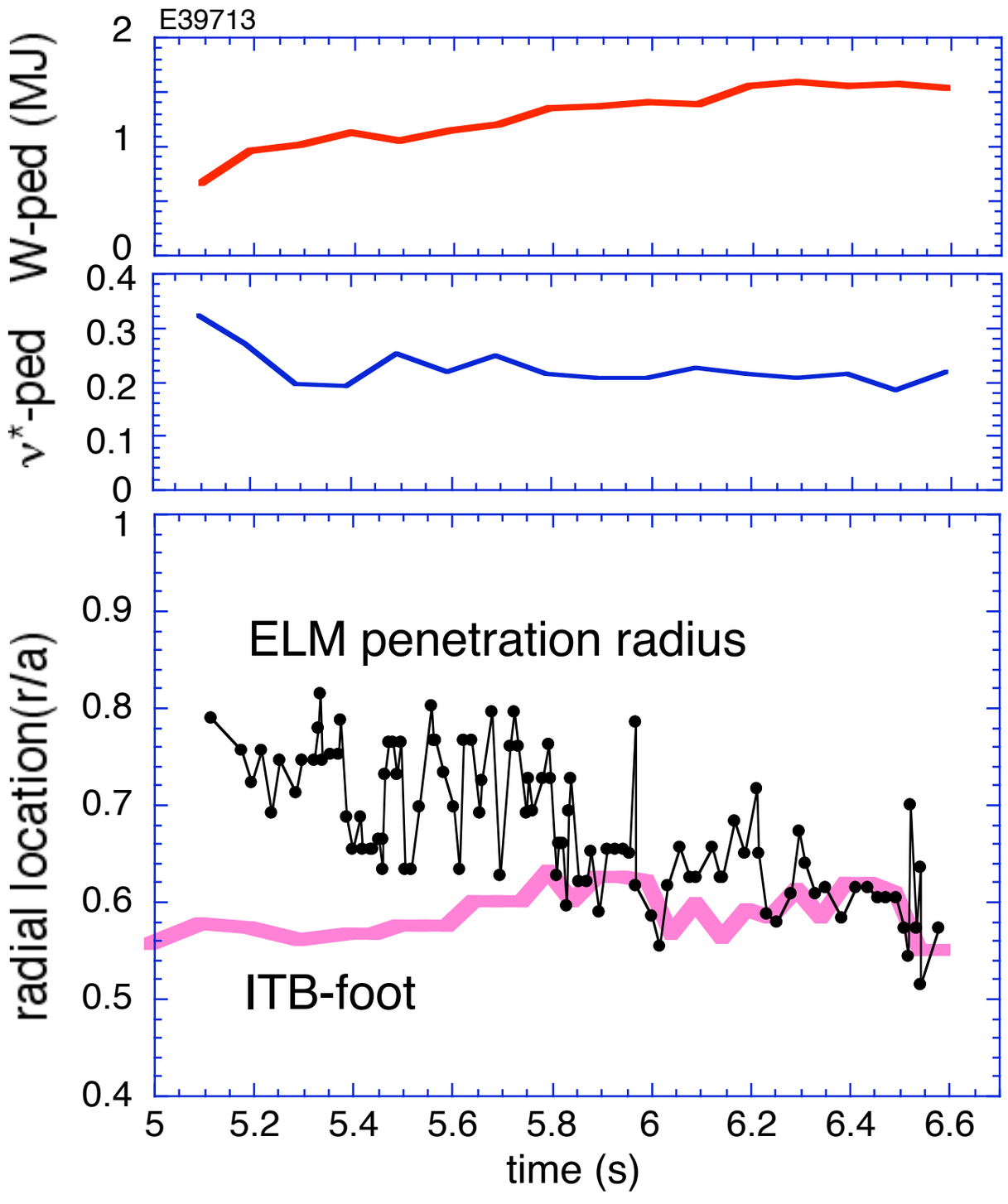

@ ELM crash depth (within 1ms):

not very regular,

tends to deepen with W-ped,

then reached the ITB-foot.

@ ITB-foot

seems to barrier the ELM crash

(5.8-5.95s,6.25-6.49s),

shrinks after a few ELM attack

(5.95s-6.0s, 6.49s-6.6s).

ELM crash depth follows ITB-foot.

Y. Kamada:

Contents & Main Results

JT-60U

1. Contribution of Pedestal to the integrated performance

Pedestal stored energy is ~20% of total stored energy in high-βp H and RS H.
Fusion Performance G Increasing with Pedestal Pressure.

2. Pedestal βp increases with total βp

At high-δ, pedestal βp increases with βp-total (both type I and Grassy).
Same tendency for standard H & ITB+H discharges.
In RS ELMy H discharges, similar to the positive shear, βp-ped-max increases with δ, and βp-ped increases with βp-tot on the same line with positive shear (except Ip=0.8MA high q95 (=8-9).
When plotted versus βp+li/2, scatter is similar.
Reason of Gradual Pedestal Evolution is not clear.

3. Compatibility of Type I ELM & ITB

Up to Ip=1.5MA, ITB has not been degraded by type I ELM crash in JT-60U
The maximum stored energy Wmax was limited by NTMs.
At higher Ip=1.8MA, Wmax was degraded without NTMs.
<= ITB shrinks by ELM crash.
Full Noninductive CD with ITB (High βp ELMyH) at Ip=1.8MA:
ELM crash depth deepens with increasing W-ped, then reaches the ITB-foot.
ITB-foot seems to barrier the ELM crash, and shrinks after a few ELM attack, and ELM crash depth follows ITB-foot.

Electron Temperature Comparisons

- Comparisons between predicted pedestal temperature and experimental electron pedestal temperature

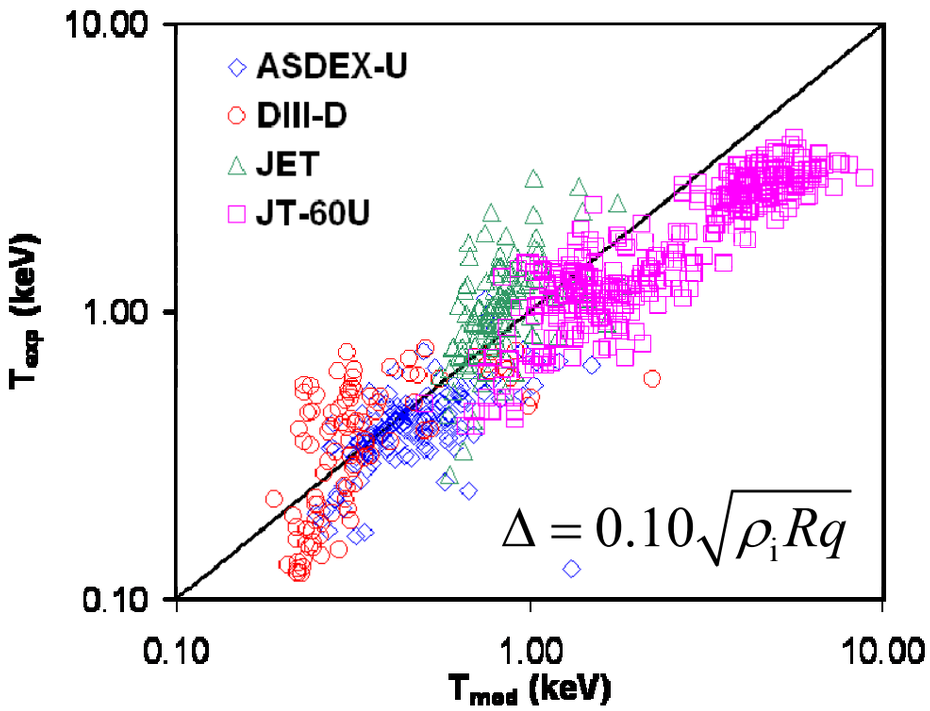

RMSE = 44%, R^2 = 0.8

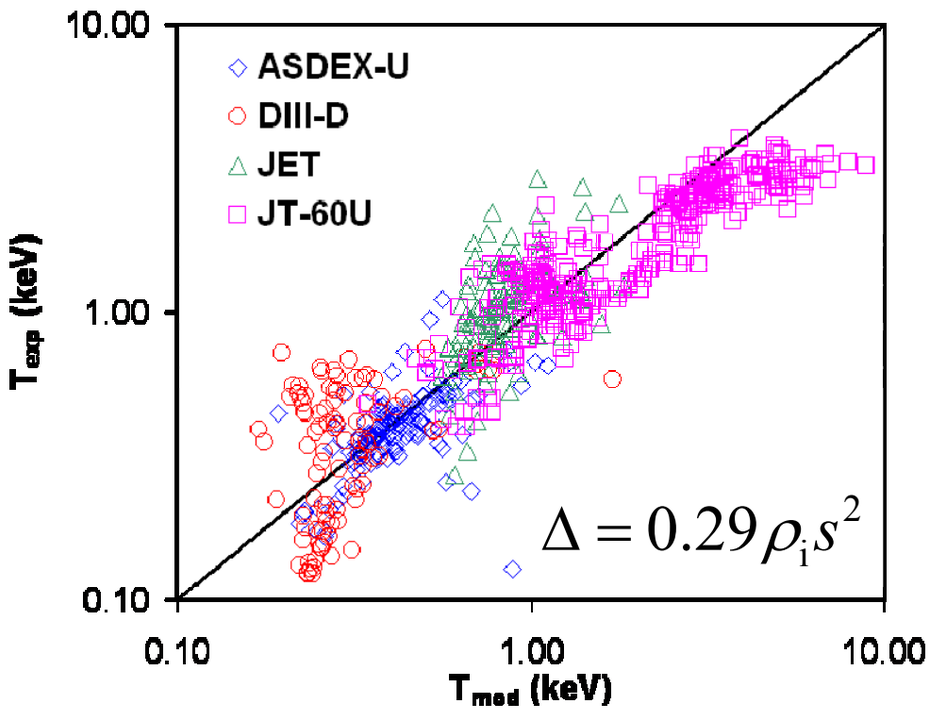

RMSE = 37%, R^2 = 0.8

ITER Predictions as a Function of n_{ped}

Ion pedestal temperature

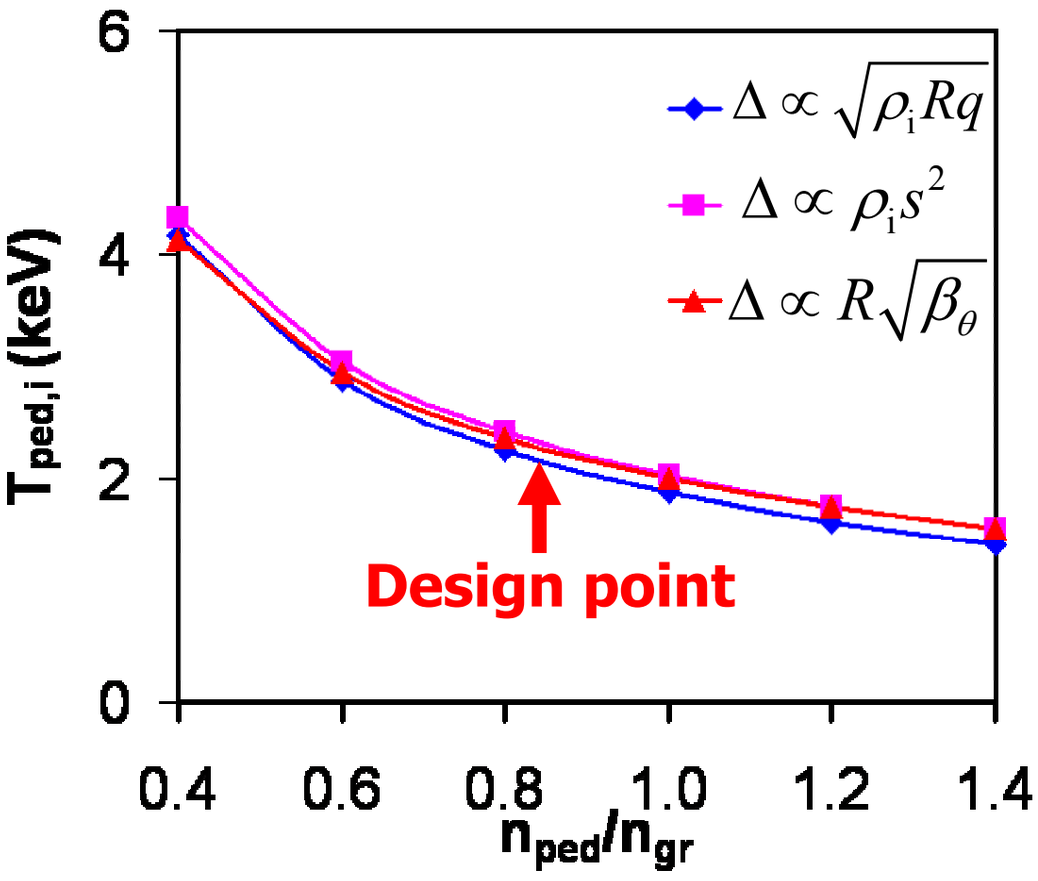

Electron pedestal temperature

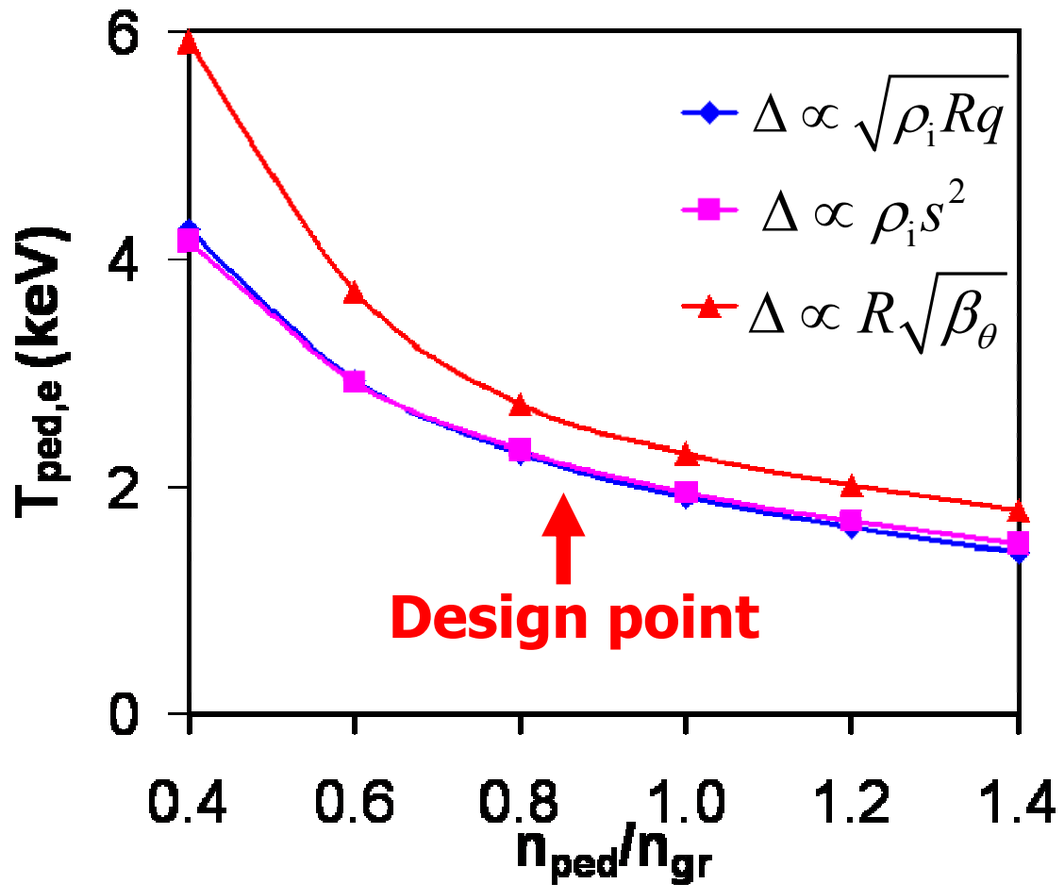

- The pedestal width ranges between 2-3 cm

Summary-II

- Models predict T_{ped} , Δ, and dp/dr in a reasonable range compared with high resolution pedestal data
  - T_{ped} in the range of 57% - 63%
  - Δ in the range of 30% - 38%
  - dp/dr in the range of 51% - 56%
- At the design point, predictions of ITER
  - Both electron and ion pedestal temperature are in the range of 2.3 to 2.5 keV
  - Pedestal width is in the range of 2-3 cm

D.C. McDonald: The impact of error models on scalings from multi-machine H-mode threshold experiments

MATHEMATICAL FORMALISM

- As example, take IAEA04R [4, 5] with physics model

$$P = f(\mathbf{x};\mathbf{c}) = c_1 \cdot S^{c_2} \cdot B^{c_3} \cdot n^{c_4}$$

where $\mathbf{x} = (S, B, n)$ and c_j, $j = 1, \cdots, J = 4$, are fitted parameters.

- Fits produced by Maximum-Likelihood method, with likelihood

$$p(\mathbf{P} \mid \mathbf{x}, \mathbf{c}) \propto \left(\prod_{i=1}^{I} {\sigma_{eff,i}}^{-1} \right) \cdot \exp\left(-\tfrac{1}{2} \chi^2 \right)$$

where,

$$\chi^2 = \sum_{i=1}^{I} \frac{\left(P_i - f(\mathbf{x}_i;\mathbf{c})\right)^2}{{\sigma_{eff,i}}^2}, \qquad {\sigma_{eff,i}}^2 = {\sigma_{p,i}}^2 + \sum_{j=1}^{J} \left(\frac{\partial f(\mathbf{x}_i;\mathbf{c})}{\partial x_{i,j}} \right)^2 {\sigma_{i,j}}^2,$$

$\sigma_{P,i}$ = errors in P, $\sigma_{i,j}$ = errors in $x_{i,j}$, and $i = 1,..., I = 1248$ label experiments.

D.C. McDonald:

ERRORS AND CONFIDENCE

- Errors calculated (Table 4) assuming given statistical model is correct
- OLS, EVOR and M-L differ significantly $\Rightarrow$ statistical model is important in final fit
- Correlation of variables in IAEA04R (Figure 4) enhances this effect

Statistical model	c_1	c_S	c_B	c_n	χ^2_N	P_{ITER}
OLS	**7.7 ± 0.3**	**0.80 ± 0.01**	**0.65 ± 0.03**	**0.44 ± 0.03**	**7.43**	**35.6**
EVOR	**7.5 ± 0.3**	**0.85 ± 0.02**	**0.58 ± 0.03**	**0.56 ± 0.03**	**7.09**	**43.4**
M-L	**6.0 ± 0.3**	**0.96 ± 0.02**	**0.45 ± 0.04**	**0.80 ± 0.05**	**6.26**	**59.0**

Table 4: *Summary of fits for selected statistical models.*

OLS: Ordinary Least Squares
EVOR: Errors-in-Variable Orthogonal Regression
M-L: Maximm-Likelihood method

D.C. McDonald:

CONCLUSIONS

- Standard Ordinary Least Squares log-linear fits for P_{L-H} assume
  - i. P errors >> errors on independent variables
  - ii. Relative errors same for all experiments
  - iii. Logs of measurements are normally distributed

- Maximum-Likelihood method
  - shows all three above assumptions bias the fit
  - provides an improved method for fitting
  - still shows that physics-statistical model does not fully describe data

- For ITER
  - OLS tends to underestimate P_{L-H}
  - Confidence interval taken may be too small
  - Further study of statistical model is required

Modeling

- **ITB Modeling**
  - Validation of ITB model with ITB width (Hayashi)
  - ITB bifurcation, oscillation (Fukuyama)
- **ELM Modeling**
  - Pedestal formation and ELM cycles (Bateman)
  - Integrated modeling of ETB and ELMs (Pankin)
  - Simulation of ELM dynamics (Kochergov)
- **ETB Modeling**
  - ETB formation in limiter tokamak (Kalupin)
  - H-mode plasma including ETB (Kalupin)
  - Edge E_r generation and dynamics (Rognlien)
  - Dynamic transport simulation (Fukuyama)

ITB Modeling

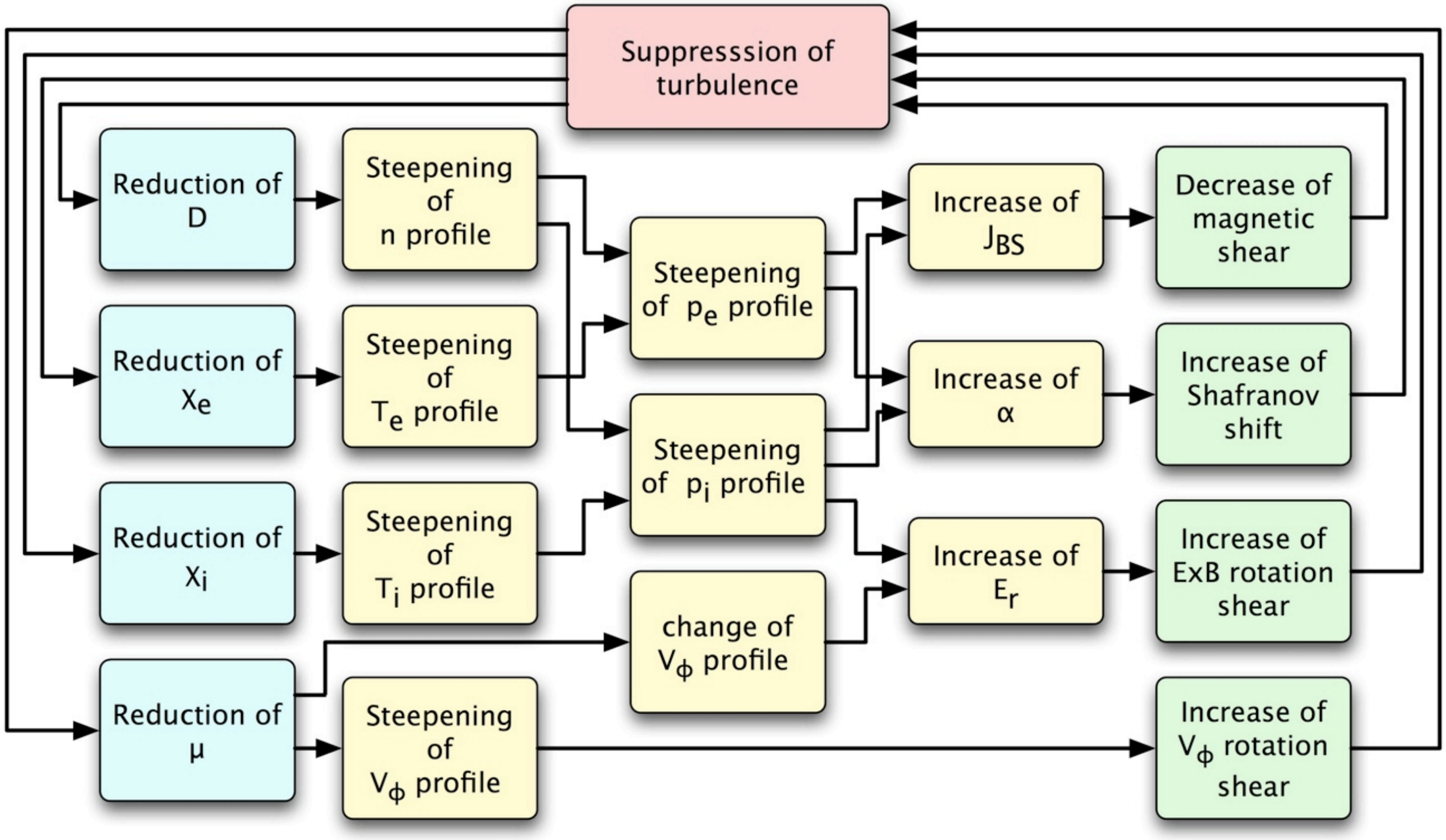

Transport modeling and simulation of box-type ITB in JT-60U RS (current-hole) plasmas (Hayashi, NF05)

Sharp reduction of anomalous transport in RS region (k~0) can reproduce JT-60U experiment.

→ Transport becomes neoclassical-level in RS region, which results in the autonomous formation of ITB and strong RS through large bootstrap current.

$$\chi_{ano} = \chi_0 F(s - k\alpha)$$

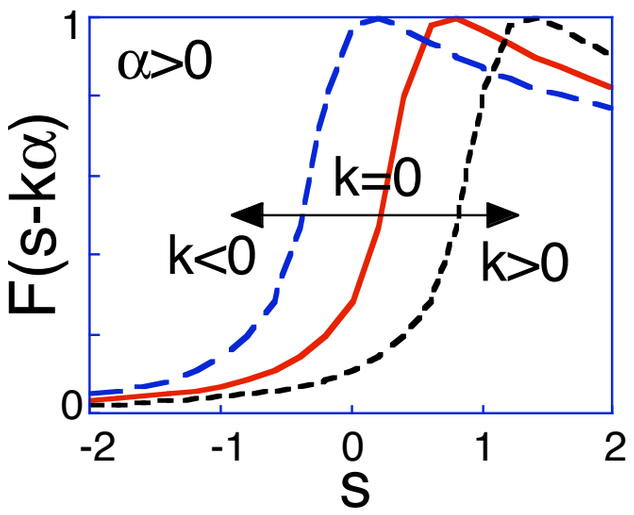

(F with k=1 : CDBM)

Inside CH region :
Current limit model based on ATMI equilibrium

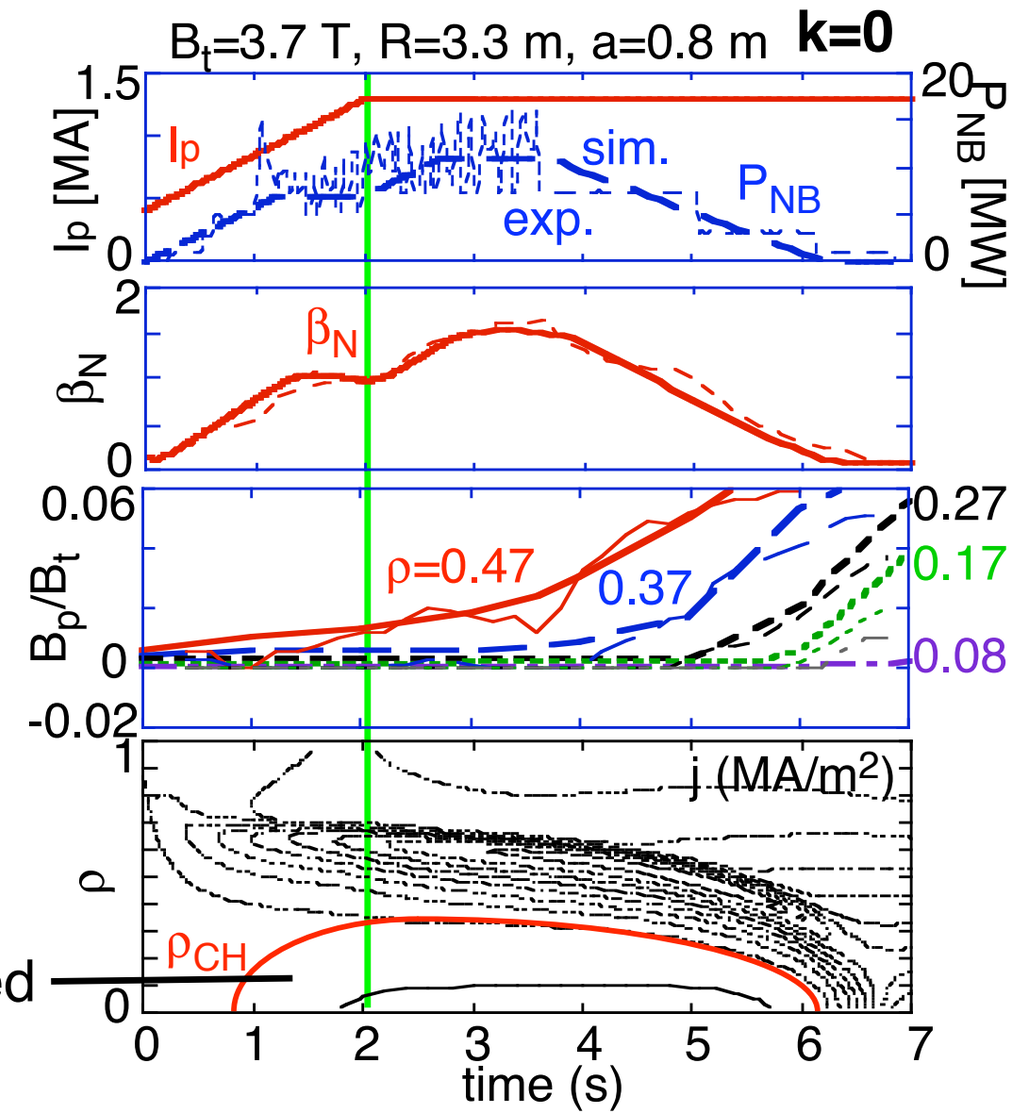

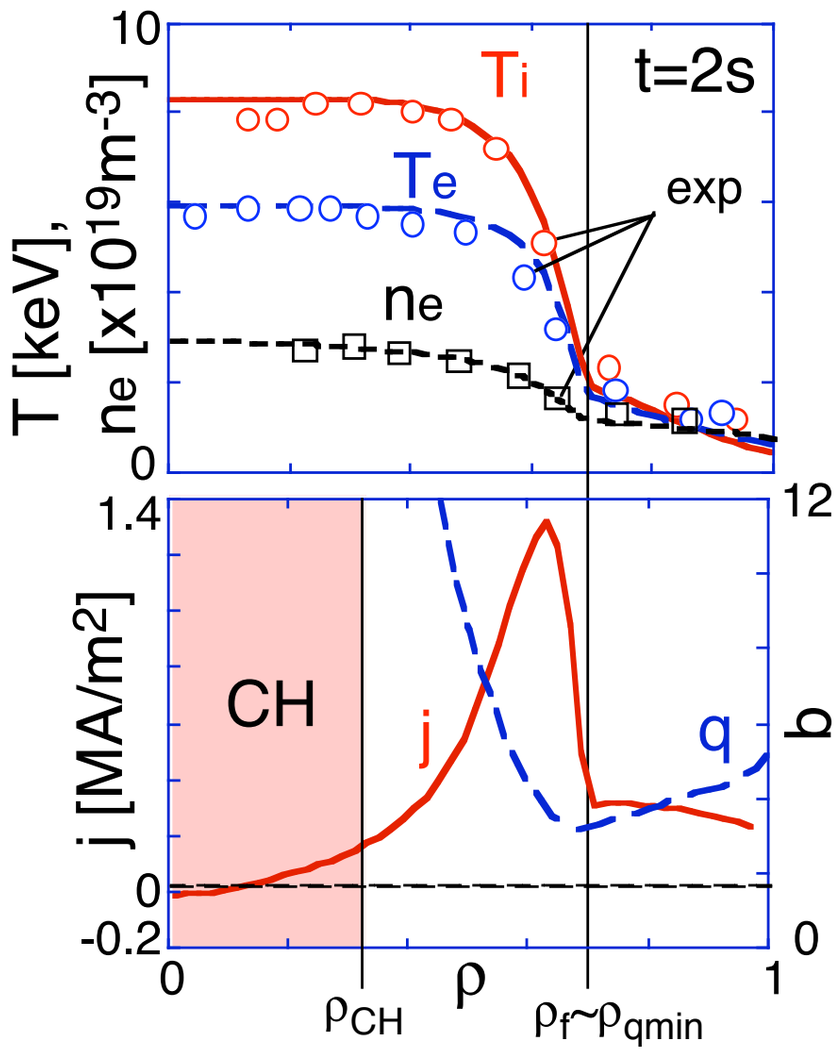

CDBM Transport Model: CDBM05

- **Thermal Diffusivity** (Marginal: $\gamma = 0$)

$$\chi_{\mathrm{TB}} = F(s, \alpha, \kappa, \omega_{\mathrm{E1}})\, \alpha^{3/2} \frac{c^2}{\omega_{\mathrm{pe}}^2} \frac{v_{\mathrm{A}}}{qR}$$

Magnetic shear	$s \equiv \dfrac{r}{q}\dfrac{\mathrm{d}q}{\mathrm{d}r}$
Pressure gradient	$\alpha \equiv -q^2 R \dfrac{\mathrm{d}\beta}{\mathrm{d}r}$
Elongation	$\kappa \equiv b/a$
$E \times B$ **rotation shear**	$\omega_{\mathrm{E1}} \equiv \dfrac{r^2}{s v_{\mathrm{A}}} \dfrac{\mathrm{d}}{\mathrm{d}r}\dfrac{E}{rB}$

- **Weak and negative magnetic shear, Shafranov shift, elongation, and $E \times B$ rotation shear reduce thermal diffusivity.**

$s - \alpha$ dependence of $F(s, \alpha, \kappa, \omega_{\mathrm{E1}})$

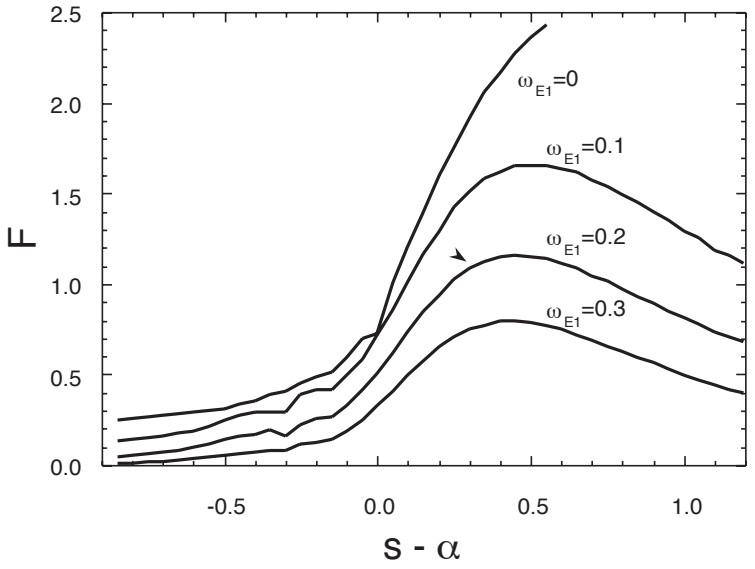

$$F(s, \alpha, \kappa, \omega_{\mathrm{E1}}) = \left(\frac{2\kappa^{1/2}}{1+\kappa^2}\right)^{3/2} \times \begin{cases} \dfrac{1}{1+G_1\omega_{\mathrm{E1}}^2} \dfrac{1}{\sqrt{2(1-2s')(1-2s'+3s'^2)}} & \text{for} \quad s' = s-\alpha < 0 \\ \dfrac{1}{1+G_1\omega_{\mathrm{E1}}^2} \dfrac{1+9\sqrt{2}s'^{5/2}}{\sqrt{2}(1-2s'+3s'^2+2s'^3)} & \text{for} \quad s' = s-\alpha > 0 \end{cases}$$

Bifurcation in Transport Barrier Formation

- **Transition in barrier formation is soft or hard?**
  - **Analysis of ITB based on CDBM model**: *Fukuyama et al. (2002)*
    - — **Constant heating power** P_{H}: Heat flux:

$$q_{\mathrm{H}} = -n\chi\frac{\mathrm{d}T}{\mathrm{d}r} = \frac{P_{\mathrm{H}}}{4\pi^2 rR}$$

    - — Pressure gradient:

$$\alpha = -q^2 R\,\frac{\mathrm{d}\beta}{\mathrm{d}r} = nq^2 R\,\frac{2\mu_0}{B^2}\left(1+\frac{1}{\eta_{\mathrm{T}}}\right)\frac{\mathrm{d}T}{\mathrm{d}r}, \qquad \eta_{\mathrm{T}} = \frac{\mathrm{d}\ln T}{\mathrm{d}\ln n}$$

    - — Thermal diffusivity:

$$\chi_{\mathrm{TB}} = C\frac{F(s,\alpha)}{1+G\omega_E^2}\,\alpha^{3/2}\,\frac{c^2}{\omega_{\mathrm{pe}}^2}\,\frac{v_{\mathrm{A}}}{qR}$$

  - Therefore

$$\frac{P_{\mathrm{H}}}{4\pi^2 rR} = n(\chi_{\mathrm{TB}}+\chi_{\mathrm{NC}})\frac{\mathrm{d}T}{\mathrm{d}r}$$

Condition of Bifurcation

- We plot α satisfying $\hat{P}_{\rm H} = (\hat{\chi}_{\rm TB} + \hat{\chi}_{\rm NC})\alpha$ as a function of $\hat{P}_{\rm H}$
  - $P_{\rm H}$ and χ are normalized by $P_{\rm H0} = 2\pi^2 \dfrac{r}{qR}\dfrac{B^2}{\mu_0}\dfrac{\eta_{\rm T}}{1+\eta_{\rm T}}\chi_0$, and $\chi_0 = C\dfrac{c^2}{\omega_{\rm pe}^2}\dfrac{v_{\rm A}}{qR}$.
- When $s \gtrsim 1$, hard transtion occurs.

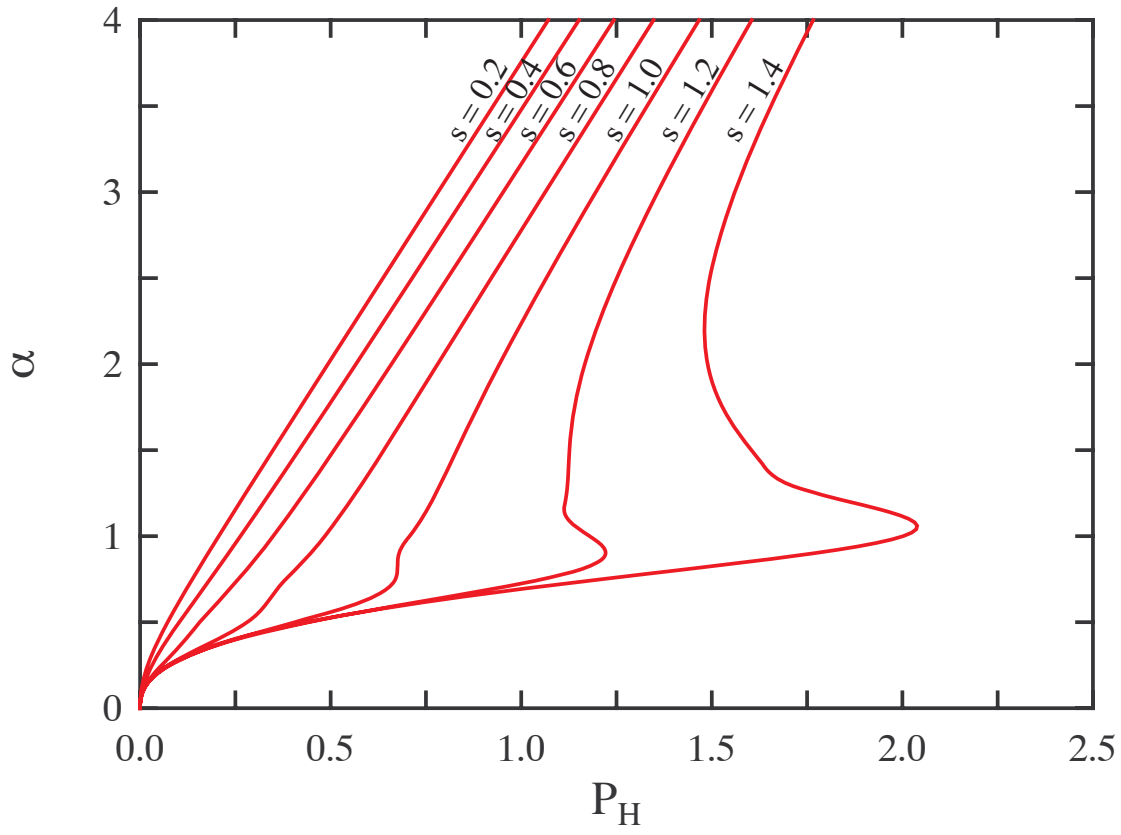

High β_p mode

- $R = 3\,\mathrm{m}$, $a = 1.2\,\mathrm{m}$, $\kappa = 1.5$, $B_0 = 3\,\mathrm{T}$, $I_p = 1\,\mathrm{MA}$
- one second after heating power of $P_H = 20\,\mathrm{MW}$ was switched on

Temperater profile

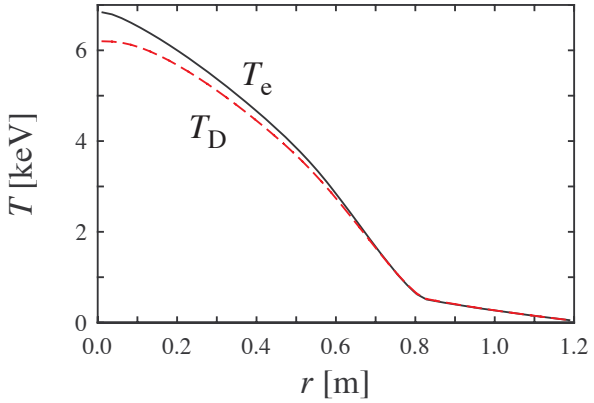

Current profile

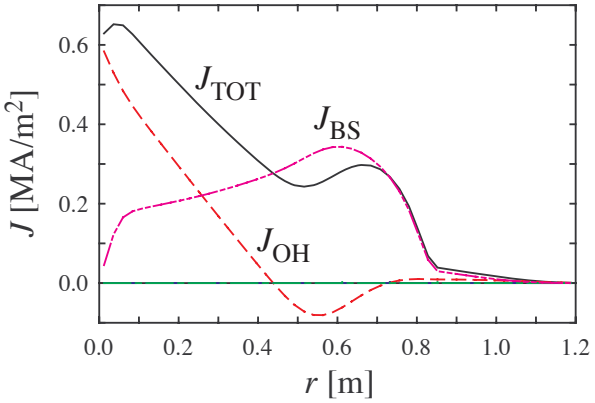

Safety factor

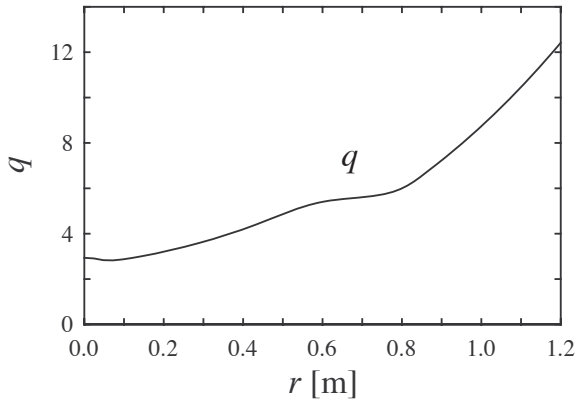

Shear and pressure

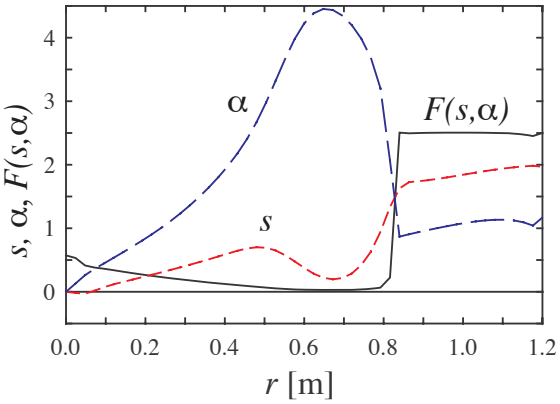

Thermal diffusivity

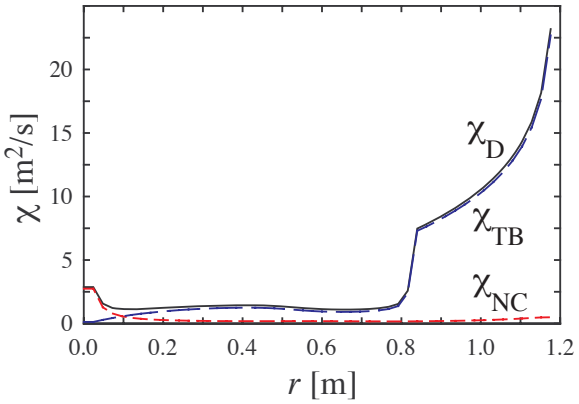

$s - \alpha$ diagram

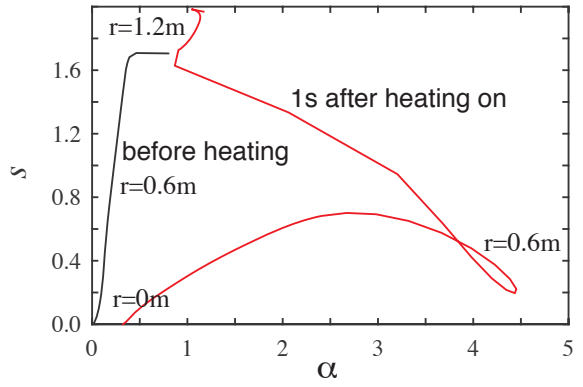

Time Evolution of High β_p mode

- $P_H = 20\,\mathrm{MW}$

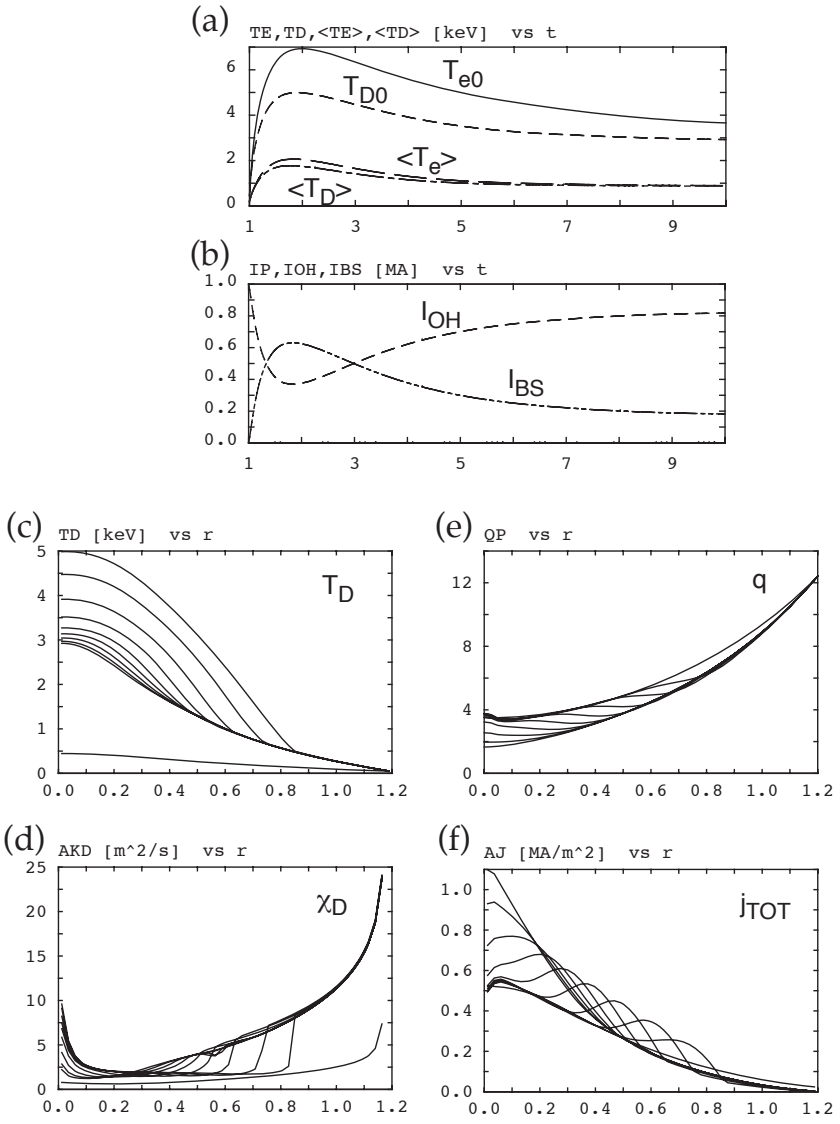

- $P_H = 24.2\,\mathrm{MW}$

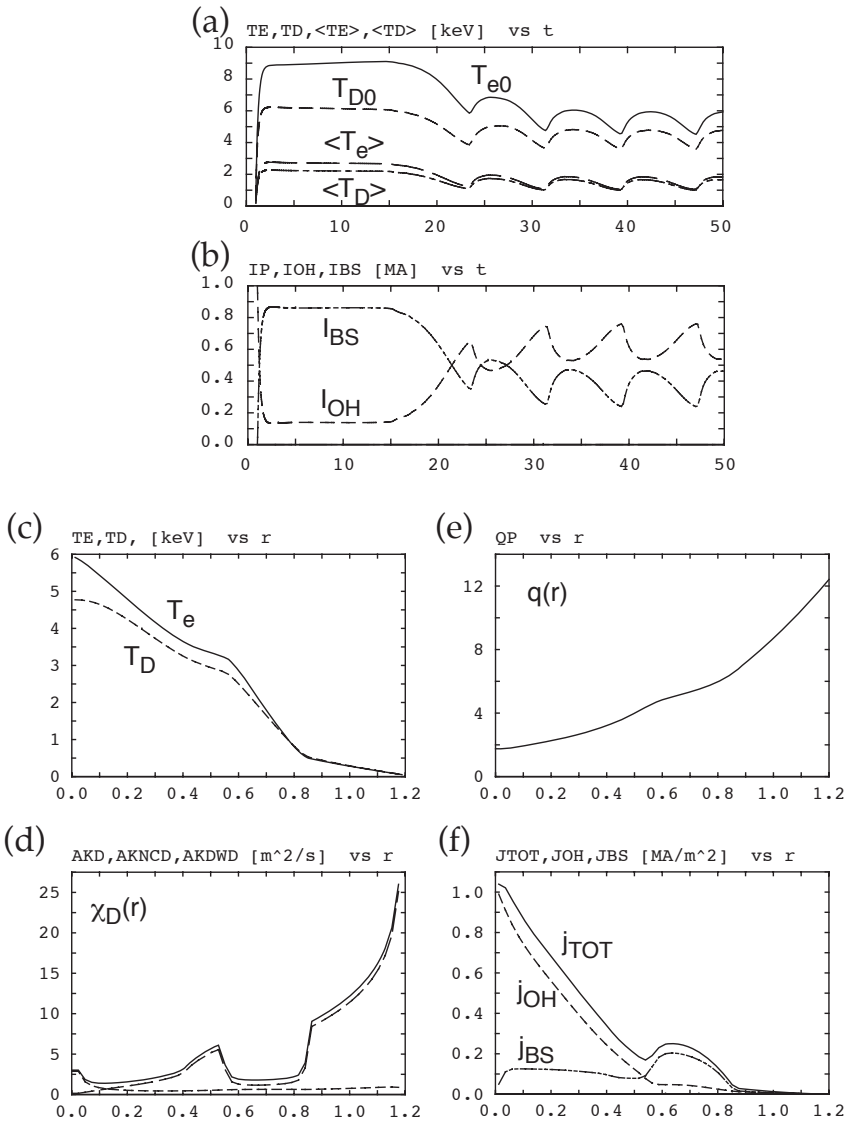

Fukuyama et al. NF (1995)

ETB Modeling

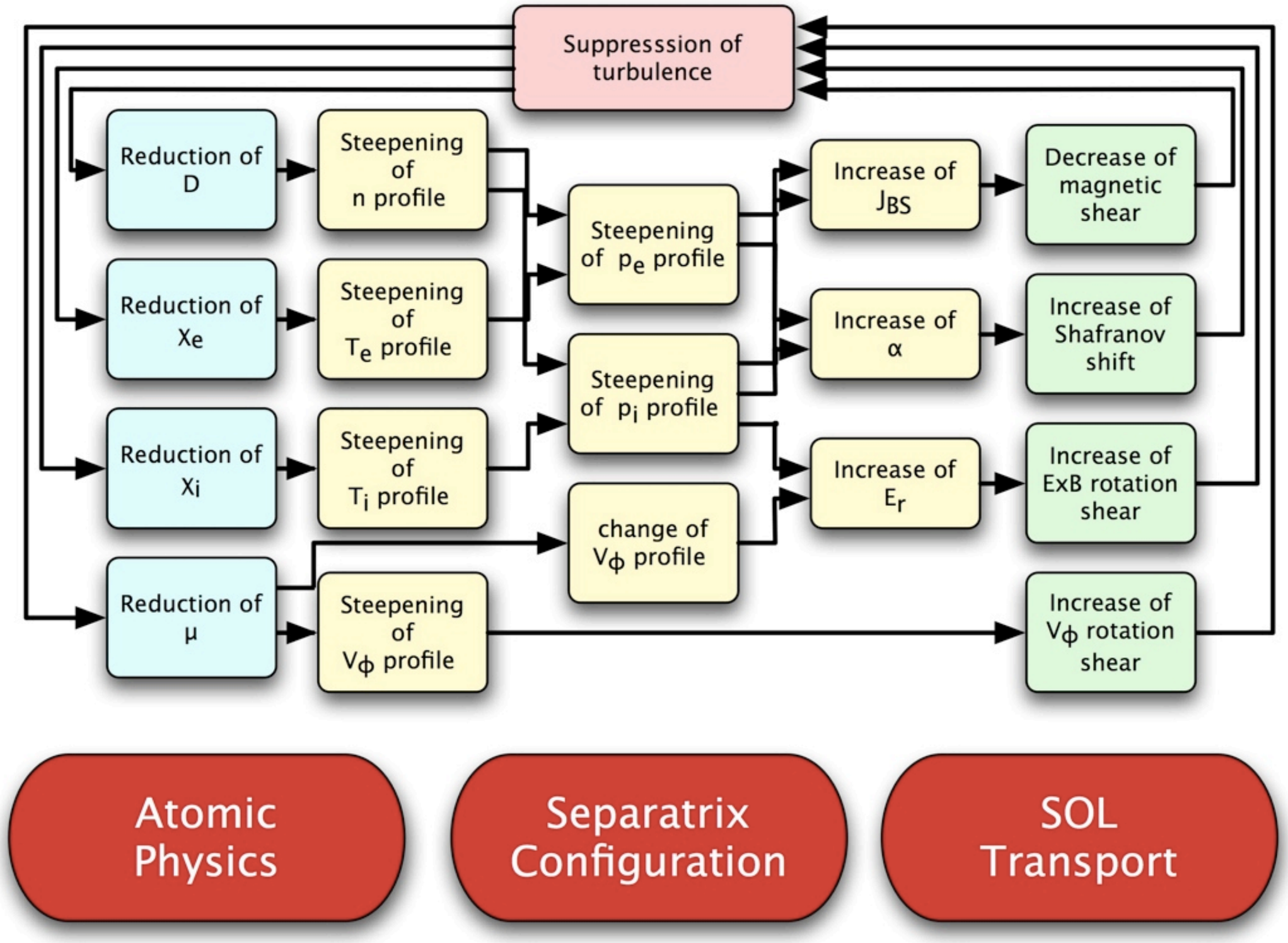

Modeling of ETB Formation

- **Transport Simulation including Core and SOL Plasmas**
  - **Role of Separatrix**
    - — Closed magnetic surface $\Longleftrightarrow$ Open magnetic field line
    - — Difference of dominant transport process
  - **Radial Electric Field**
  - **Poloidal rotation, Toroidal rotation**
  - **Atomic Processes**

- **1D Transport code** (TASK/TX) *Fukuyama et al. PPCF (1994)*
  - **Two fluid equation for electrons and ions**
    - — Flux surface averaged
    - — Coupled with Maxwell equation
    - — Neutral diffusion equation
  - **Neoclassical transport**
  - **Turbulent transport**
    - — Current diffusive ballooning mode
    - — Ambipolar diffusion through poloidal momentum transfer
    - — Thermal diffusivity, Perpendicular viscosity

Model Equation (1)

- **Fluid equations** (electrons and ions)

$$\frac{\partial n_s}{\partial t} = -\frac{1}{r}\frac{\partial}{\partial r}(r n_s u_{sr}) + S_s$$

$$\frac{\partial}{\partial t}(m_s n_s u_{sr}) = -\frac{1}{r}\frac{\partial}{\partial r}(r m_s n_s u_{sr}^2) + \frac{1}{r} m_s n_s u_{s\theta}^2 + e_s n_s (E_r + u_{s\theta} B_\phi - u_{s\phi} B_\theta) - \frac{\partial}{\partial r} n_s T_s$$

$$\frac{\partial}{\partial t}(m_s n_s u_{s\theta}) = -\frac{1}{r^2}\frac{\partial}{\partial r}(r^2 m_s n_s u_{sr} u_{s\theta}) + e_s n_s (E_\theta - u_{sr} B_\phi) + \frac{1}{r^2}\frac{\partial}{\partial r}\left(r^3 n_s m_s \mu_s \frac{\partial}{\partial r}\frac{u_{s\theta}}{r}\right)$$

$$+ F_{s\theta}^{\mathrm{NC}} + F_{s\theta}^{\mathrm{C}} + F_{s\theta}^{\mathrm{W}} + F_{s\theta}^{\mathrm{X}} + F_{s\theta}^{\mathrm{L}}$$

$$\frac{\partial}{\partial t}\left(m_s n_s u_{s\phi}\right) = -\frac{1}{r}\frac{\partial}{\partial r}(r m_s n_s u_{sr} u_{s\phi}) + e_s n_s (E_\phi + u_{sr} B_\theta) + \frac{1}{r}\frac{\partial}{\partial r}\left(r n_s m_s \mu_s \frac{\partial}{\partial r} u_{s\phi}\right)$$

$$+ F_{s\phi}^{\mathrm{C}} + F_{s\phi}^{\mathrm{W}} + F_{s\phi}^{\mathrm{X}} + F_{s\phi}^{\mathrm{L}}$$

$$\frac{\partial}{\partial t}\frac{3}{2} n_s T_s = -\frac{1}{r}\frac{\partial}{\partial r} r\left(\frac{5}{2} u_{sr} n_s T_s - n_s \chi_s \frac{\partial}{\partial r} T_{\mathrm{e}}\right) + e_s n_s (E_\theta u_{s\theta} + E_\phi u_{s\phi})$$

$$+ P_s^{\mathrm{C}} + P_s^{\mathrm{L}} + P_s^{\mathrm{H}}$$

Neoclassical Transport Model

- **Neoclassical transport**
  - Viscosity force arises when plasma rotates in the poloidal direction.
  - Banana-Plateau regime

$$F_{s\theta}^{\mathrm{NC}} = -\sqrt{\pi} q^2 n_s m_s \frac{v_{\mathrm{T}s}}{qR} \frac{\nu_s^*}{1+\nu_s^*} u_{s\theta}$$

$$\nu_{\mathrm{s}}^* \equiv \frac{\nu_s qR}{\epsilon^{3/2} v_{\mathrm{T}s}}$$

- **This poloidal viscosity force induces**
  - Neoclassical radial diffusion
  - Neoclassical resistivity
  - Bootstrap current
  - Ware pinch

Turbulent Transport Model

- **Turbulent Diffusion**
  - Poloidal momentum exchange between electron and ion through the turbulent electric field
  - Ambipolar flux (electron flux = ion flux)

$$F_{\mathrm{i}\theta}^{\mathrm{W}} = - \; F_{\mathrm{e}\theta}^{\mathrm{W}}$$

$$= - ZeB_{\phi} n_{\mathrm{i}} D_{\mathrm{i}} \left[-\frac{1}{n_{\mathrm{i}}} \frac{dn_{\mathrm{i}}}{dr} + \frac{Ze}{T_{\mathrm{i}}} E_r - \left\langle \frac{\omega}{m} \right\rangle \frac{ZeB_{\phi}}{T_{\mathrm{i}}} - \left(\frac{\mu_{\mathrm{i}}}{D_{\mathrm{i}}} - \frac{1}{2} \right) \frac{1}{T_{\mathrm{i}}} \frac{dT_{\mathrm{i}}}{dr} \right]$$

- **Perpendicular viscosity**
  - Non-ambipolar flux (electron flux ≠ ion flux): $\mu_s = \text{constant} \times D$
- **Diffusion coefficient** (proportional to $|E|^2$)
  - Current-diffusive ballooning mode turbulence model

Model of Scrape-Off Layer Plasma

- **Particle, momentum and heat losses along the field line**
  - Decay time

$$\nu_{\mathrm{L}} = \begin{cases} 0 & (0 < r < a) \\ \dfrac{C_{\mathrm{s}}}{2\pi r R\{1 + \log[1 + 0.05/(r-a)]\}} & (a < r < b) \end{cases}$$

  - **Electron source term**

$$S_{\mathrm{e}} = n_0 \langle \sigma_{\mathrm{ion}} v \rangle n_{\mathrm{e}} - \nu_{\mathrm{L}} (n_{\mathrm{e}} - n_{\mathrm{e,div}})$$

- **Recycling from divertor**
  - Recycling rate: $\gamma_0 = 0.8$
  - Neutral source

$$S_0 = \frac{\gamma_0}{Z_{\mathrm{i}}} \nu_{\mathrm{L}} (n_{\mathrm{e}} - n_{\mathrm{e,div}}) - \frac{1}{Z_{\mathrm{i}}} n_0 \langle \sigma_{\mathrm{ion}} v \rangle n_{\mathrm{e}} + \frac{P_{\mathrm{b}}}{E_{\mathrm{b}}}$$

- **Gas puff from wall**

Typical Profiles without Turbulent Transport

$$n_e \quad E_r \quad n_i - n_e$$
$$u_{er} \quad u_{e\theta} \quad u_{e\phi}$$
$$j_\phi \quad n_0 \quad T_e$$

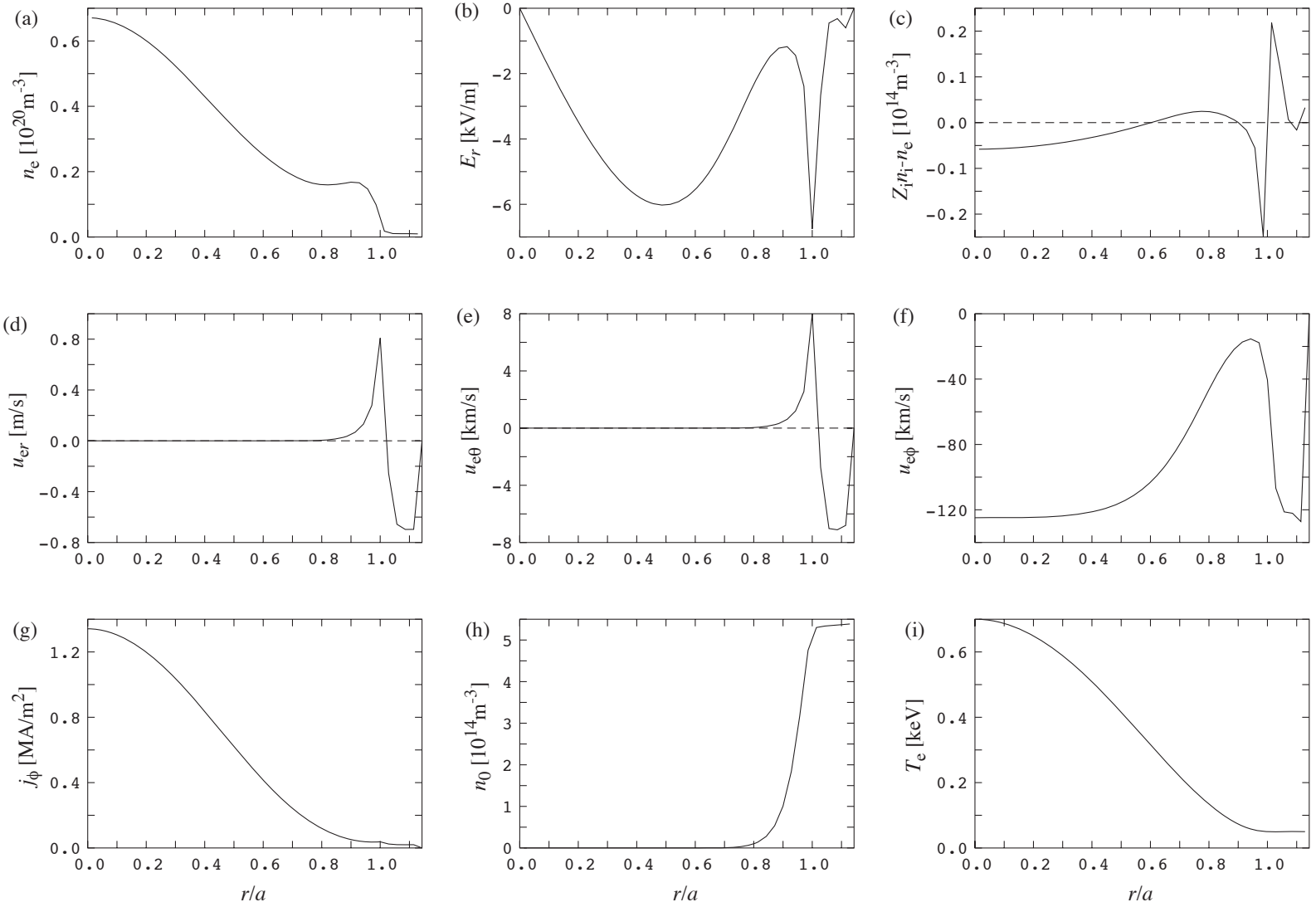

ETB formation

Edge Temperature Dependence

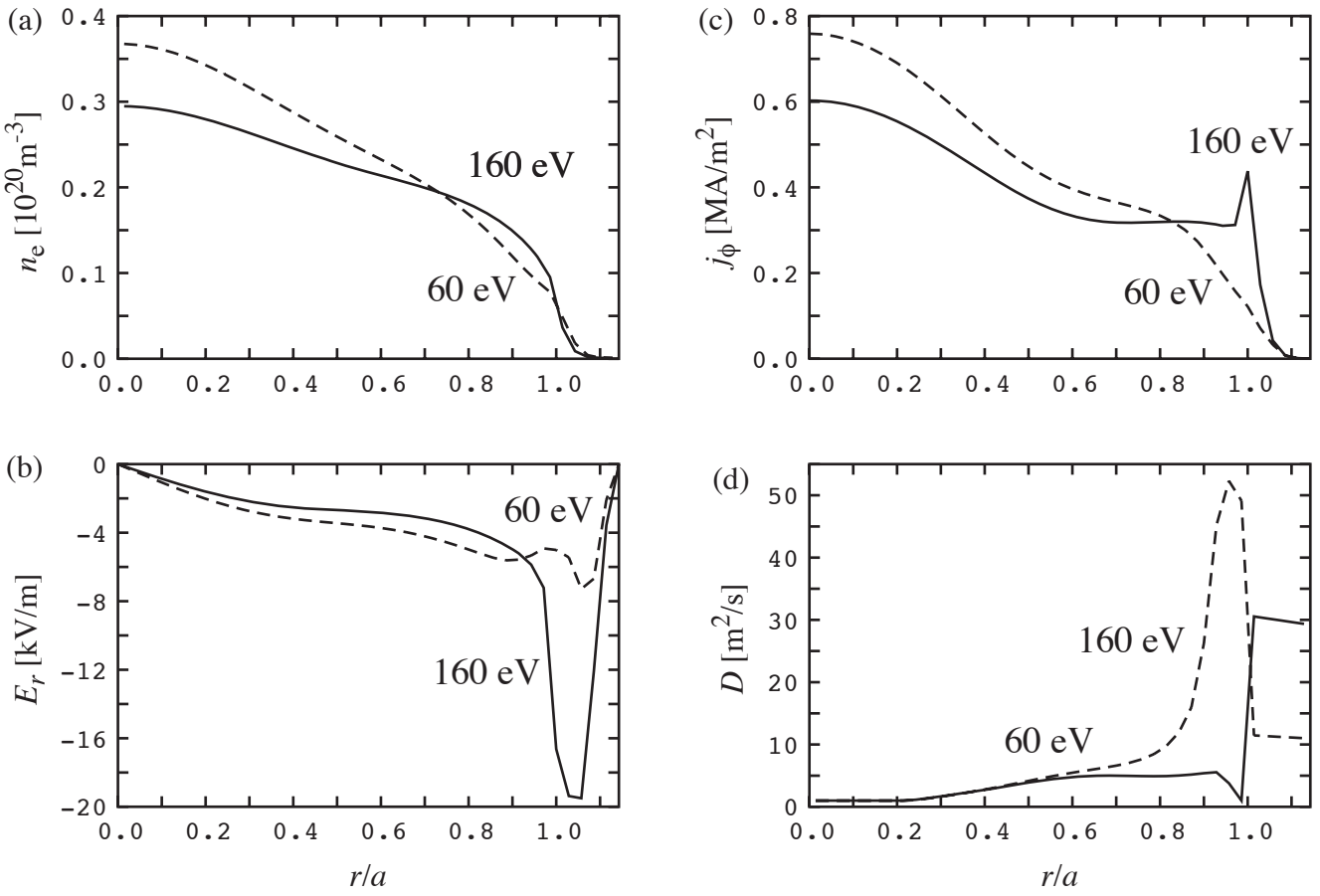

Simulation of plasma rotation and radial electric field

- **JFT-2M parameter**: NBI co-injection $\longrightarrow$ counter-injection
- Toroidal rotation $\Longrightarrow$ Negative E_r $\Longrightarrow$ Density peaking
- **TASK/TX**: Particle Diffusivity: $0.3\,\mathrm{m}^2/\mathrm{s}$, Ion viscosity: $10\,\mathrm{m}^2/\mathrm{s}$

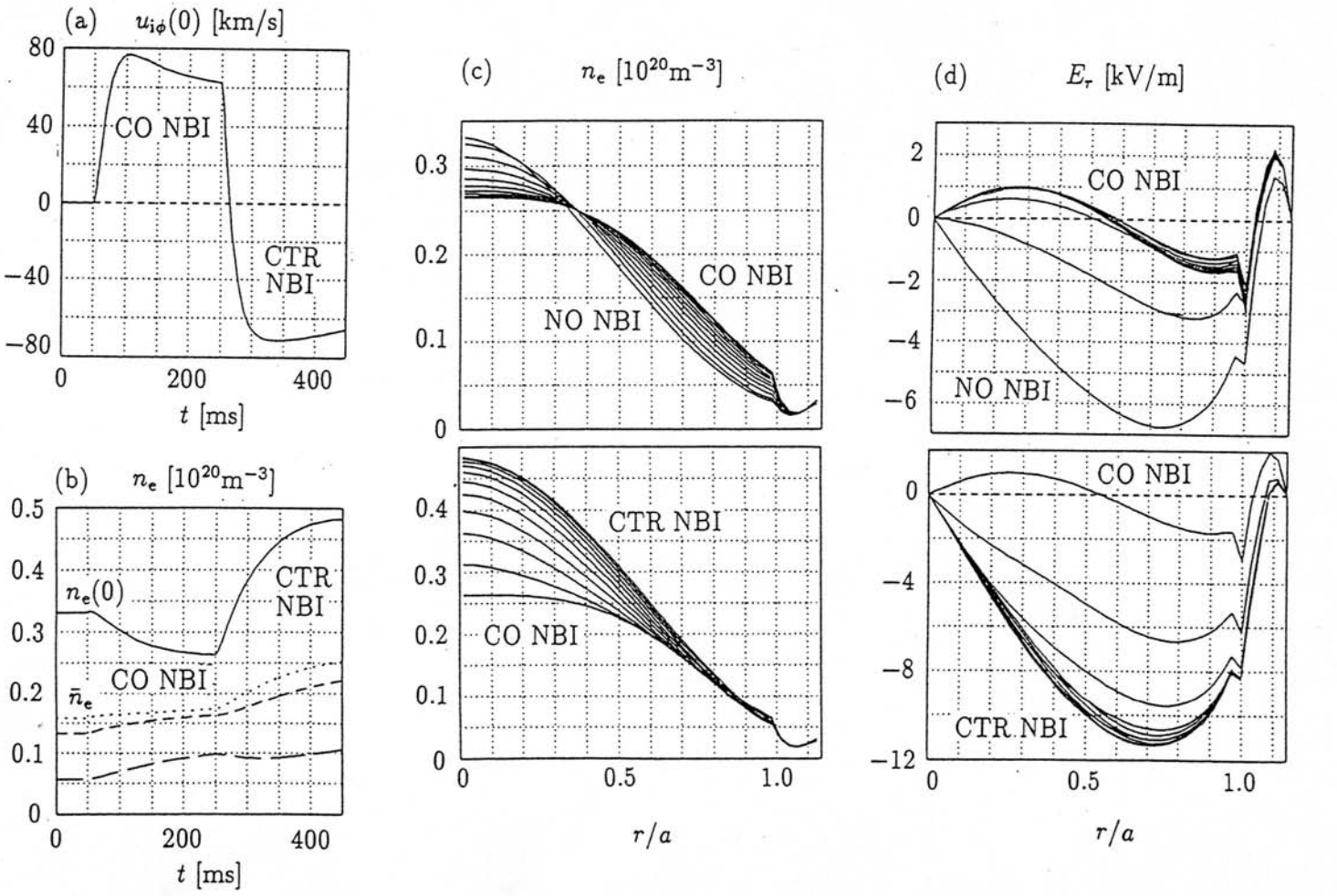

ELM Modeling

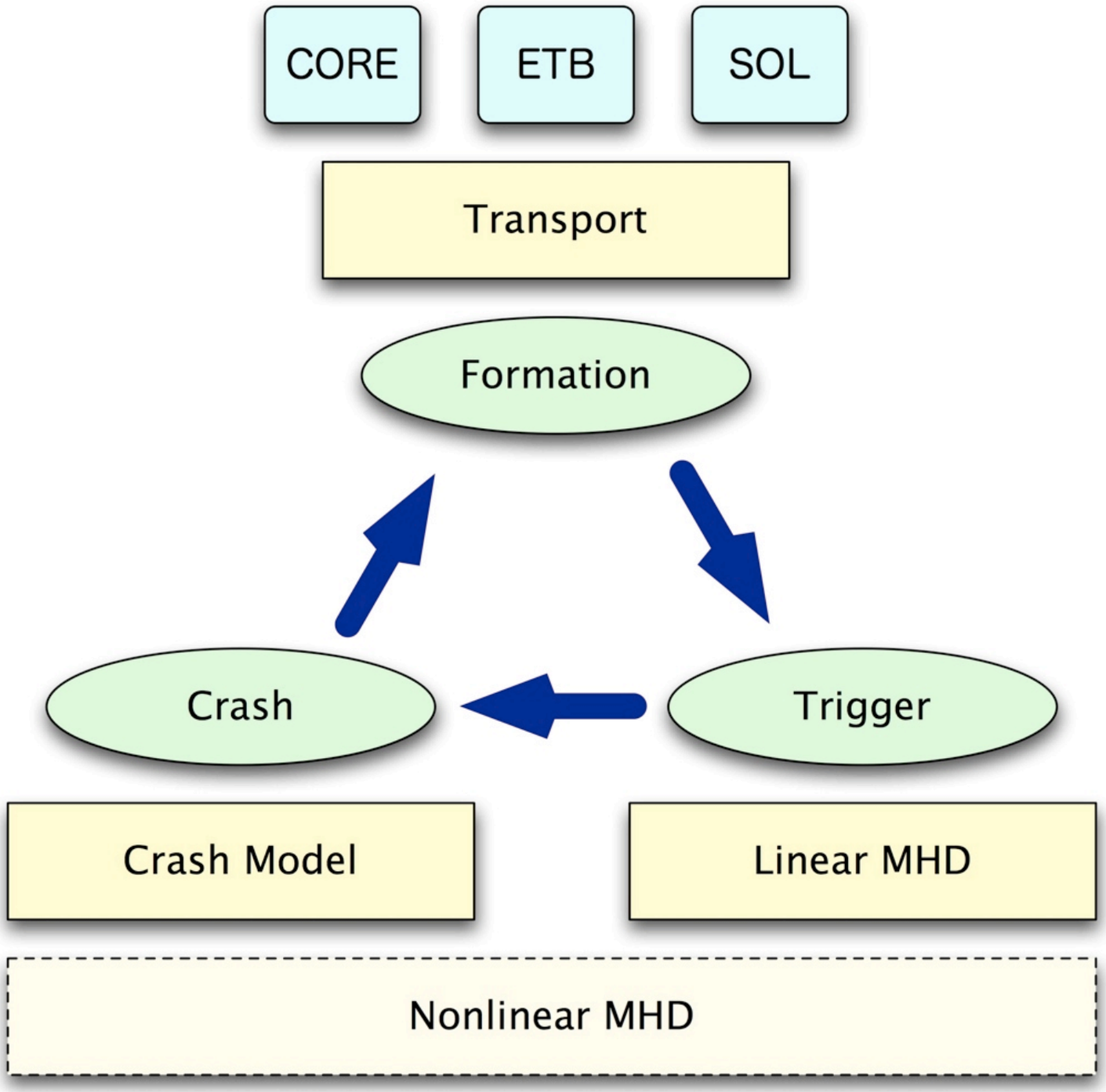

R. Bateman:

Static ETB model

Predictions for ITER Performance

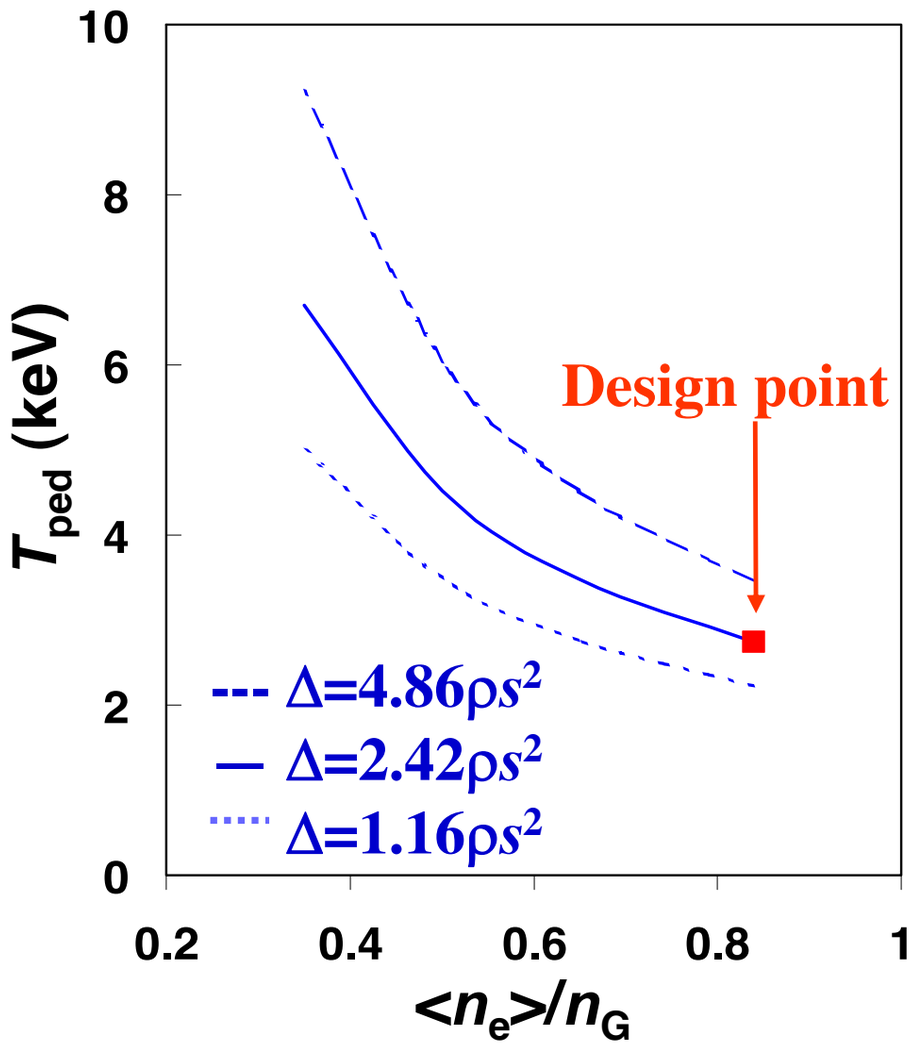

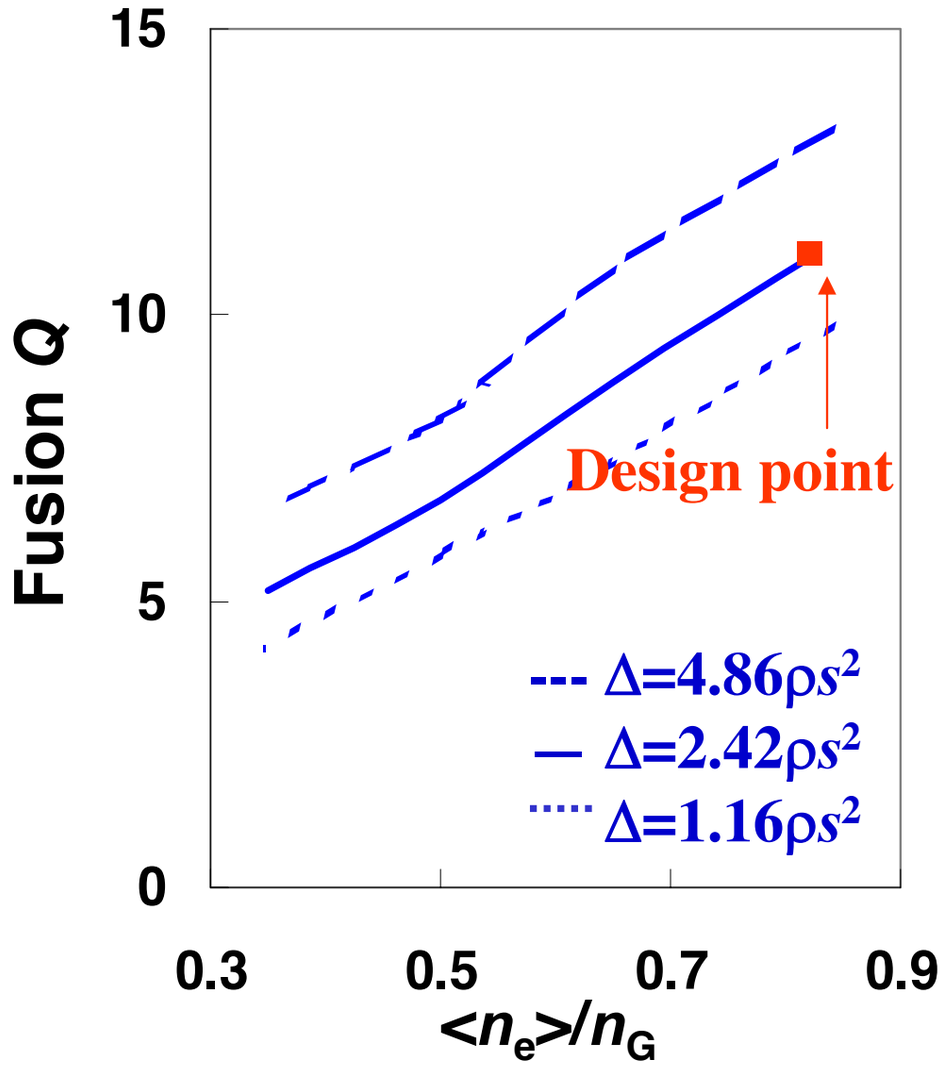

Integrated Predictive Modeling Simulations of Burning Plasma Experiment Designs, Plasma Phys. Control. Fusion, 45 (2003) 1939, by G. Bateman, T. Onjun, and A. H. Kritz.

LEHIGH UNIVERSITY

R. Bateman:

Dynamic ETB model

Predicted Fusion Q for ITER

- **Models used in JETTO simulations:**
  - **Mixed-Bohm/gyro-Bohm transport model**
  - **Dynamic model for pedestal and ELMs**
- **Models used in BALDUR simulations**
  - **Multi-Mode (MMM95) transport model**
  - **Pedestal temperature from JETTO simulations provide boundary condition in the BALDUR code**
- **Predicted values of fusion** $Q \equiv 5\,P_\alpha / (P_{aux} + P_\Omega)$
  - **JETTO and BALDUR simulations agree within error bounds**

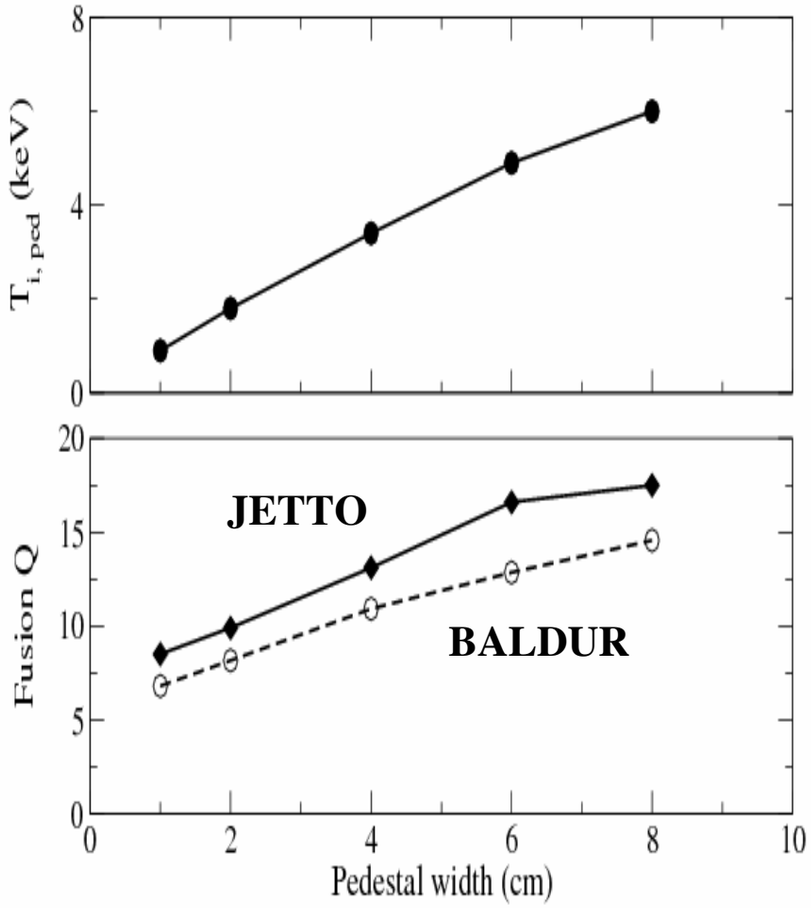

- **HELENA and MISHKA stability analyses carried out**
  - **Profiles and equilibrium obtained from JETTO just before ELM crash**

MHD-calibrated edge localized mode model in simulations of ITER, Phys. Plasmas, 12, 082513 (2005), by Onjun, Bateman, Kritz and V. Parail.

LEHIGH UNIVERSITY

W.A. Houlberg, J.E. Kinsey:
IAEA2004

Edge T fixed

ITER-SS simulation with GLF23

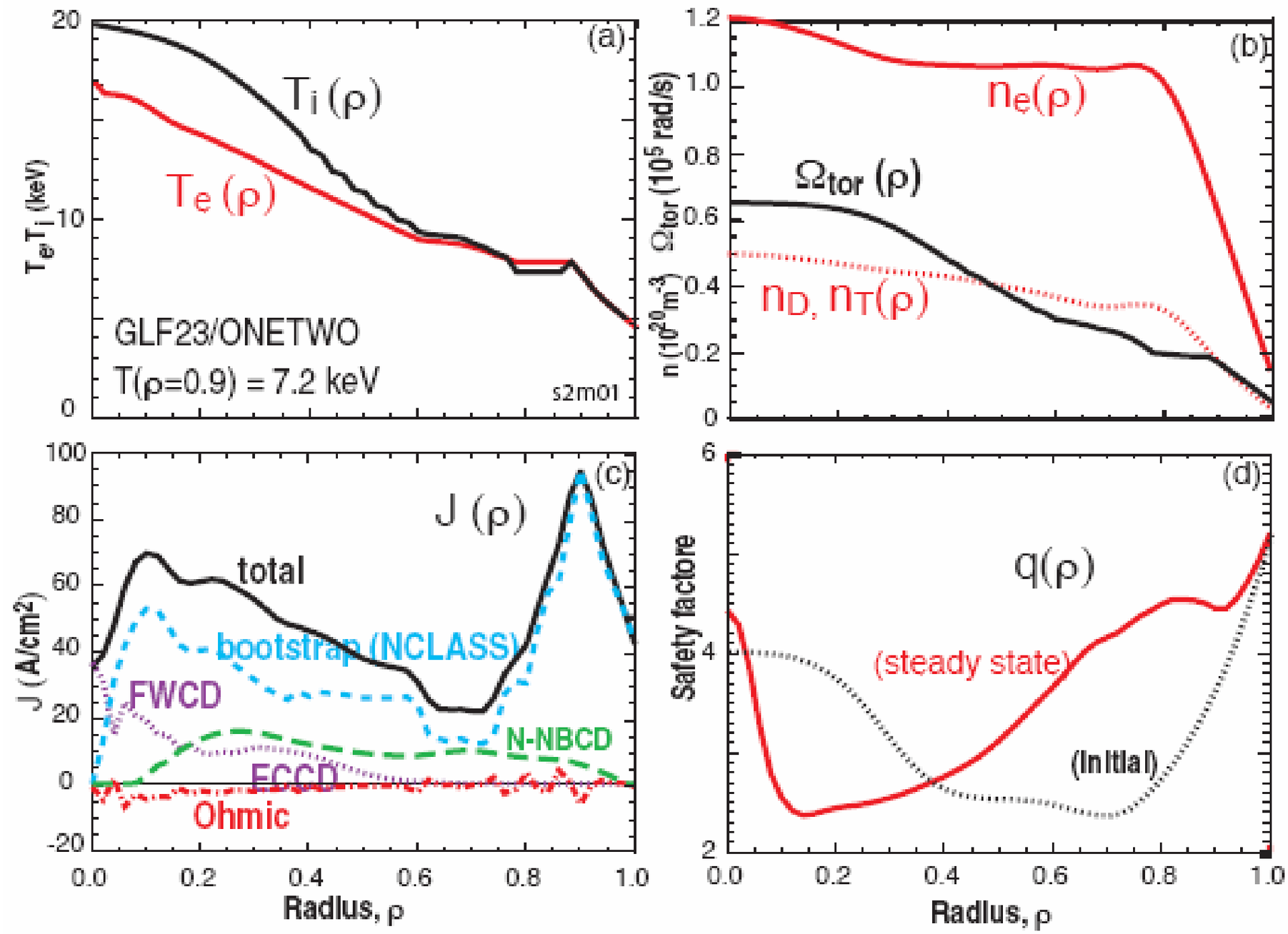

Figure 3: The profiles for ITER steady-state scenario 4 [1] from the ONETWO code with the GLF23 transport model: a) temperatures, b) densities and toroidal rotation, c) current contributions, and d) the initial and final q profiles.

Edge T fixed

ITER simulation with CDBM

High Q

CDBM05

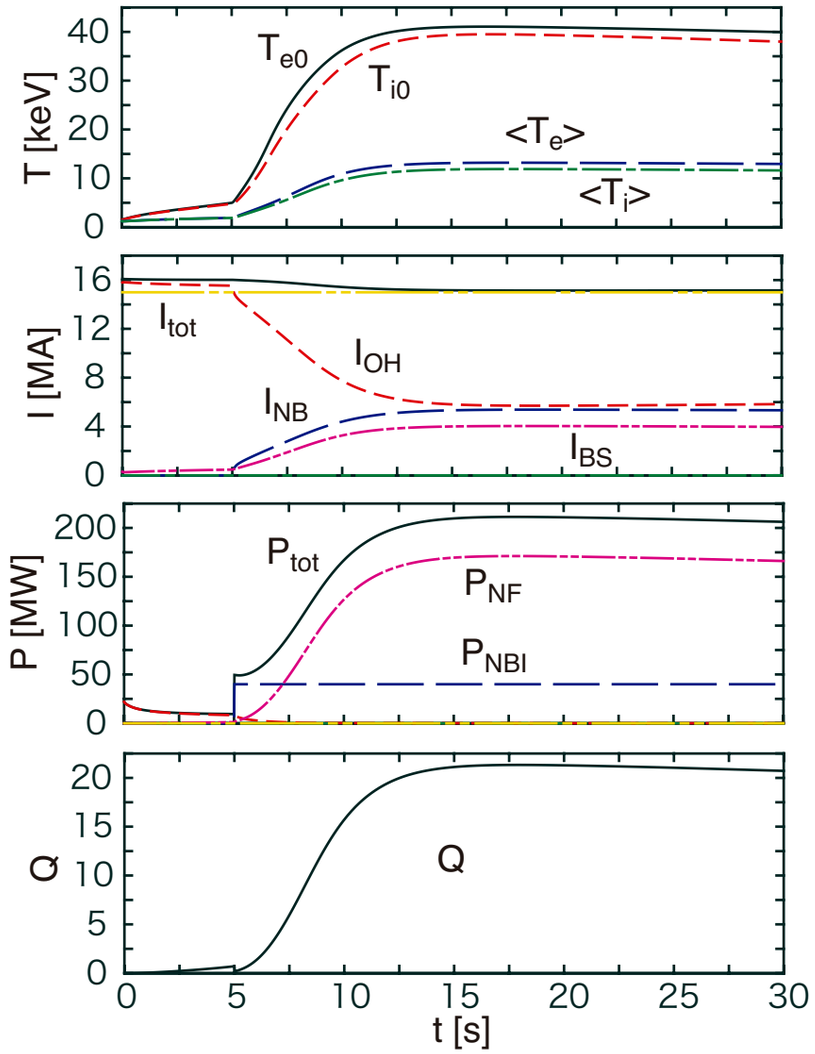

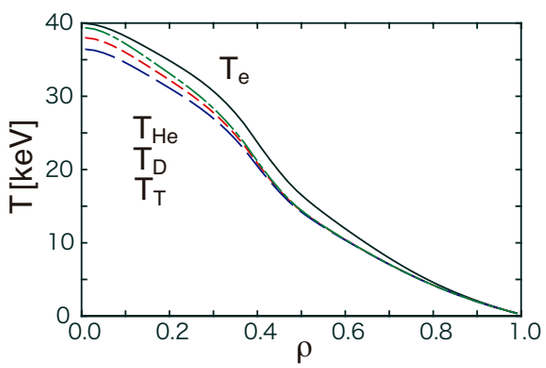

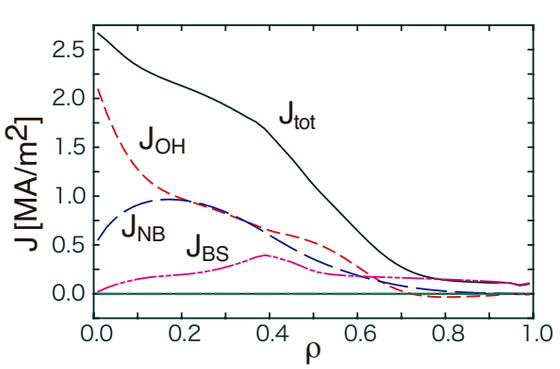

Steady State

CDBM05

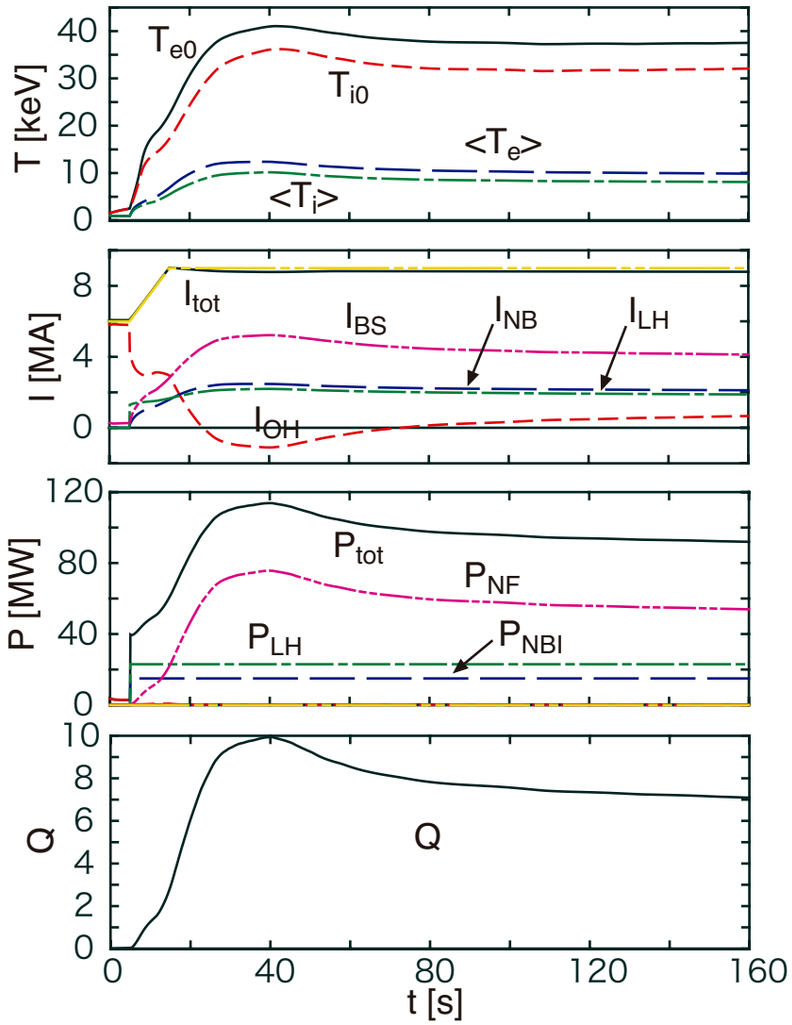

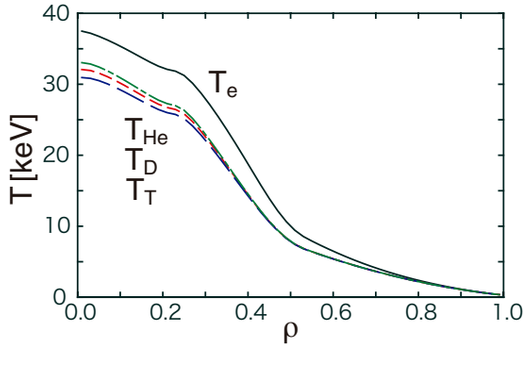

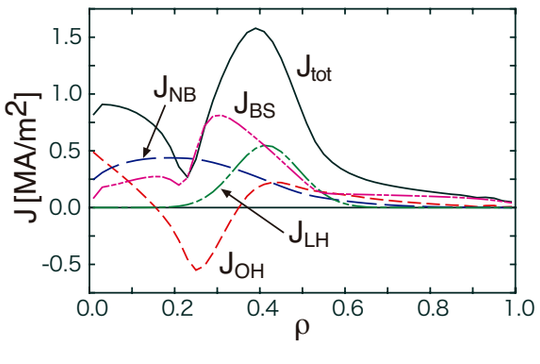

$P_{NB} = 15$ MW

$P_{LH} = 23$ MW

R. Bateman:

Elements of an Integrated Tokamak Modeling Code

- Sawtooth Region (q < 1)
- Core Confinement Region
- Magnetic Islands
- Edge Pedestal Region
- Scrape-off Layer
- Vacuum/Wall/ Conductors/Antenna

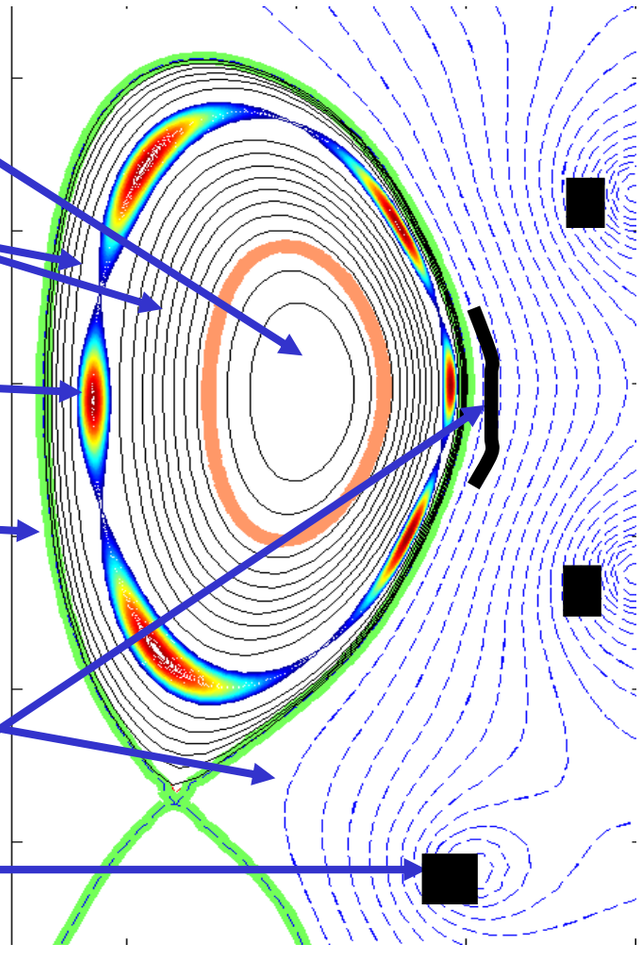

Core Transport

Edge Transport

Plasma Turbulence

MHD Equilibrium

Heating Current Drive

Atomic Physics

Radiative Transport

Large Scale Instabilities

Plasma-Wall Interactions

Structure Integrated Code TASK

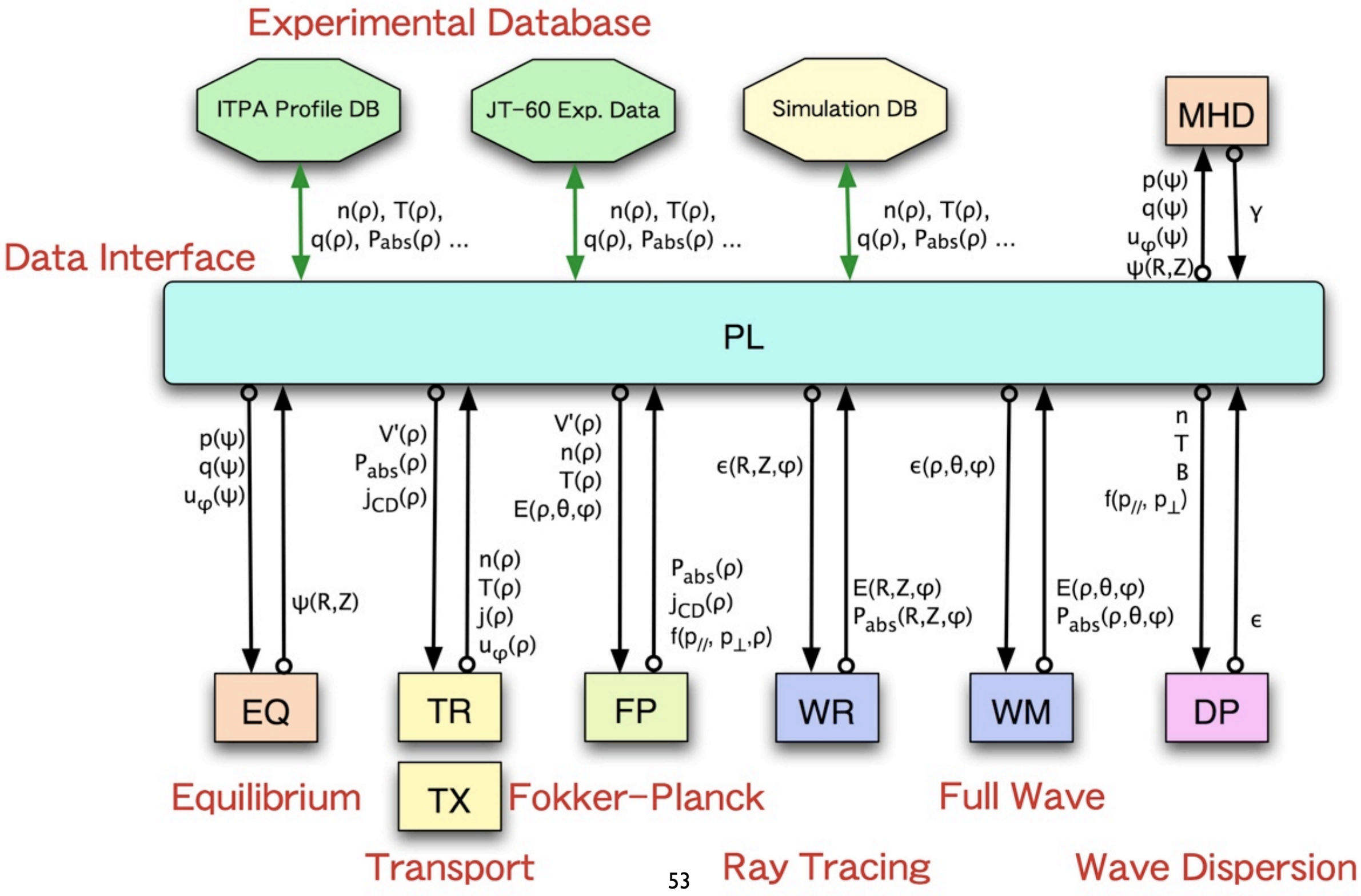

Scaling Summary

- **Scaling**
  - **H-mode global confinement scaling:**
    - The origin of β degradation and the effect of aspect ratio becomes clearer.
    - The shape factor affects the global scaling.
    - The impact of error models on scaling was extensively studied.
    - Newly-proposed scalings little affect the ITER performance.
    - The possibility of density peaking and performance improvement of ITER was pointed out.

Modeling Issues (1)

- **ITB Modeling**
  - Magnetic shear, Shafranov shift, ExB rotation shear, and V_ϕ shear are probable mechanisms of turbulence suppression.
  - Modeling including these mechanisms have been developed. More efforts to validate the model is required.
  - Projection to burning plasmas requires:
    - Self-consistent analysis of actuators
    - Compatibility with confinement of α particles and induced Alfvén eigenmodes
    - Effect of ELMs and other MHD activities.

Modeling Issues (2)

- **Particle transport modeling**
  - Modeling of density peaking and coupling to toroidal and poloidal rotations has to be validated.
- **ETB modeling**
  - Several models have been proposed.
  - Validation by systematic comparison with experimental data is strongly needed.
  - Dynamic modeling of LH transition is still required for threshold power scaling.
  - Two-dimensional and three-dimensional effects should be examined quantitatively.

Modeling Issues (3)

- **ELM modeling**
  - Significant progress has been made on the modeling of Type-I ELMs.
  - Projection to burning plasmas still requires reliable ETB models and crash models.
  - Modeling of small ELMs and control of ELMs are important for reducing the peak heat flux to the divertors.